## Title

Biosensors Fabrication by Polydimethylsiloxane Stamping and Nanostructured Platinum for Construction of Improved Reference and Sensing Electrodes



## Author

Wang, Bo

## Publication Date

2016

Peer reviewed|Thesis/dissertation

UNIVERSITY OF CALIFORNIA

Los Angeles

# Biosensors Fabrication by Polydimethylsiloxane Stamping and Nanostructured Platinum for Construction of Improved Reference and Sensing Electrodes

A dissertation submitted in partial satisfaction of the

requirements for the degree of Doctor of Philosophy

in Chemical Engineering

by

Bo Wang

2016

ABSTRACT OF THE DISSERTATION

Biosensors Fabrication by Polydimethylsiloxane Stamping and Nanostructured Platinum for Construction of Improved Reference and Sensing Electrodes

by

Bo Wang

Doctor of Philosophy in Chemical Engineering

University of California, Los Angeles, 2016

Professor Harold G. Monbouquette, Chair

The ability to monitor neuronal processes linked to complex behaviors is very important for study of neurological disorders and abnormal behaviors. The study of neurological disorders on a chemical level requires sensitive and fast techniques to monitor the release of neurotransmitters in near-real time *in vivo*. The establishment of relationships between behaviors and neurotransmitter release events will help us better decipher complex systems in the brain. This information can be obtained from near-real-time neurochemical sensing. Our lab has successfully fabricated glutamate (Glut) microbiosensors which can selectively detect glutamate in the presence of the electroactive interferents, dopamine (DA) and ascorbic acid (AA), with fast response time (~1 s), high selectivity and low detection limit. However, the enzyme transfer and immobilization steps, which are the key steps in the fabrication of our electroenzymatic glutamate biosensors, formerly were achieved by manually depositing a bovine serum albumin (BSA)/glutaraldehyde (GAH)/glutamate oxidase mixture onto the surface of the electrodes. Although the GAH crosslinking enzyme

immobilization method has been validated both *in vivo* and *in vitro*, the manual deposition procedure causes problems such as inconsistent enzyme layer thickness, which results in inconsistent sensor performance. In addition, if each microelectrode on a microelectrode array (MEA) format probe requires a different enzyme coating, manual enzyme immobilization will be difficult due to the spacing between each microelectrode (each electrode is ~40 μm apart). Thus, a non-manual method is needed to transfer enzyme to select microelectrode sites with high consistency and spatial resolution.

Microcontact printing (μCP) has been used to directly pattern arrays of proteins on silicon or glass substrates without compromising the activity of the proteins. An elastomeric polydimethylsiloxane (PDMS) stamp is covered with a solution of target protein for inking. This results in deposition of a layer of protein on the surface of the stamp. After removing excess liquid and drying, the protein can be transferred to a target substrate by stamping. The μCP approach allows reliable feature replication with dimensions down to about 500 nm. To test the feasibility of this technique for transferring enzyme to electrodes, PDMS stamping of enzyme onto disk electrode surfaces was attempted. Glucose oxidase (GOx) was chosen as a model enzyme for this work. BSA and GOx were deposited together on a PDMS stamp, transferred to an electrode surface and then crosslinked by GAH vapor treatment. The biosensor exhibited excellent performance characteristics including a linear range up to 2 mM with sensitivity of 29.4 ± 1.3 μA $mM^{-1}$ $cm^{-2}$ and detection limit of 4.3 ± 1.7 μM (S/N = 3) as well as a rapid response time of ~2 s. In comparison to those previously described, this glucose biosensor exhibits an excellent combination of high sensitivity, low detection limit, rapid response time, and good selectivity.

For the fabrication of microbiosensors, a microscale stamp was created by casting the polymer on a silicon mold that previously was micromachined. The stamp was used for

transferring glucose oxidase and choline oxidase to selected microelectrode sites on the same microprobe. As a result, a dual sensing microprobe (glucose and choline) was fabricated and tested *in vitro*. The dual sensor we fabricated showed high sensitivity for choline and glucose (286 and 117 μA/mM $cm^2$, respectively) accompanied by a low detection limit (3 and 1 μA respectively). The work presented here shows the prospect for fabricating a microelectrode array for multiple neurotransmitter sensing and high throughput enzyme deposition, which inevitably leads to the potential development of a high performance neurotransmitter sensor.

Another route to improve sensor performance is through an increase in effective electrode surface area. A platinum black (Pt black) deposit is often used for enlarging the effective electrode surface area. The nanoscopic Pt particles making up the deposit also often show improved catalytic behavior resulting in potential reduction for electrooxidations. However, practical applicability of Pt black is limited as a consequence of its low mechanical stability. In addition, Pt black has been reported to cause a cytotoxic reaction *in vivo*, as traces of lead used in the electrolyte during fabrication elute from the deposit. An alternative nanostructured Pt coating was reported recently that results in impedance reduction at small electrodes. In comparison to Pt black, all chemicals used in the alternate deposition process are non-cytotoxic. The Pt nanograss was electrodeposited onto the microelectrode surface using an aqueous solution of $H_2PtCl_6$ and formic acid. According to SEM images, Pt black was irregularly attached to the surface rather than grown from the surface while Pt nanograss showed a more uniform pillar-like structure. A choline biosensor was developed by incorporating Pt nanograss deposition which results in working potential reduction (from 0.7 V to 0.45 V). This nanostructured platinum coating was coated on both working electrode and on-probe reference electrode and characterized by scanning electron microscope (SEM). In this work, polyphenylenediamine (PPD) and Nafion were coated on electrode surface

sequentially as permselective polymers. With the developed choline sensor testing at physiological concentrations, the performance of the biosensors is quite consistent. By using external Ag/AgCl reference electrode (0.45V), the detection limit was ~2 μM with sensitivity of ~196 μA/mM $cm^2$ and response time of 3-5s. With an on-probe reference electrode (0.35 V), the detection limit was ~3 μM with the sensitivity ~123 μA/mM $cm^2$ and response time of 3-5s. Also, no responses from the electroactive interferents, such as ascorbic acid (AA), dopamine (DA), DOPA (a DA catabolite) or DOPAC (a DA precursor), over their respective physiological concentration ranges, were detected. Therefore, Pt nanograss will be an excellent substitute for Pt black for Pt surface modification with non-cytotoxic properties, which will be beneficial for *in vivo* applications.

The dissertation of Bo Wang is approved.

Kate Wassum

Tatiana Segura

Yvonne Chen

Harold G. Monbouquette, Chair

University of California, Los Angeles

2016

TABLE OF CONTENTS

LIST OF FIGURES

## LIST OF TABLES

# ACKNOWLEDGMENTS

I would like to first acknowledge my Ph.D. advisor, Professor Harold G. Monbouquette, for helping me become a better researcher throughout my graduate school career. I have learned how to set up a goal, solve a problem systematically which is something really important for the rest of my career and life. His patience, kindness, and enthusiasm for my work and my development as a graduate student are unparalleled, and I will be forever grateful for his guidance.

I would also like to thank my dissertation committee, Professor Yvonne Chen, Professor Kate Wassum and Professor Tatiana Segura, for their input and time, their comments and suggestions for my research.

Next, I would also like to thank my lab members on my projects, including Dr. Allison Yorita, Dr. Bonhye Koo, Dr. Lili Feng, Brenda Huang, and Mac Clay were all instrumental in making the lab a friendly, welcoming place where we could discuss our research and help each other out. Dr. Bonhye Koo, as my collaborator on the PDMS stamping project, was an expertise in developing the fabrication process for the mold and microstamps. I have learned a lot from her. On the Pt nanograss neurotransmitter sensors project, I collaborated with Dr. Lili Feng. I'm always impressed and influenced by her optimistic personality.

Last, but certainly not least, I would like to thank my family for being my biggest pillar of support during my graduate school career. Mom, Dad, younger brother Jucheng, my wife Jie Yan and my lovely newborn baby Ruby Wang– I could not have done this without you, and I am so grateful for your love and support.

VITA

| | |
|---|---|
| 2006 – 2010 | B.S., Pharmaceutical Sciences |
| | Peking University Health Science Center |
| | Beijing, China |
| 2010 – 2012 | M.S., Medicinal Chemistry |
| | Peking University Health Science Center |
| | Beijing, China |
| 2012 – 2014 | M.S., Chemical and Biomolecular Engineering |
| | Department of Chemical and Biomolecular Engineering, UCLA |
| | Los Angeles, CA |
| 2012 – 2016 | Graduate Student Researcher |
| | Department of Chemical and Biomolecular Engineering, UCLA |
| | Los Angeles, CA |
| 2012 – 2016 | Teaching Assistant |
| | Department of Chemical and Biomolecular Engineering |
| | Los Angeles, CA |

PUBLICATIONS AND PATENTS

1. **Bo Wang**[†], Bonhye Koo[†], Liwen Huang, Harold G. Monbouquette, "Implantable Microbiosensor Fabrication by Polydimethylsiloxane Stamping for Combined Amperometric Monitoring of Glucose and Choline", **2016**, in preparation.
2. Lili Feng, Anne Collins, Xiaona Wen, **Bo Wang**, K.M. Wassum, and Harold G. Monbouquette "Implantable Microprobe with Arrayed Microsensors for Amperometric Monitoring of

Choline", **2016**, in preparation.

3. **Bo Wang**†, Lili Feng†, Bonhye Koo, Harold G. Monbouquette, "A High Performance All-in-one Electroenzymatic Choline Microsensor by Introducing Nanostructured Platinum", **2016**, in preparation.
4. **Bo Wang**, Bonhye Koo, Harold G. Monbouquette, "Enzyme Deposition by Polydimethylsiloxane Stamping for Biosensor Fabrication", **2016**, in preparation.
5. Yin Tang, Yang-Bing Li, **Bo Wang**, Ri-Yuan Lin, Mallory van Dongen, Danielle M. Zurcher, Xiao-Yan Gu, Mark M. Banaszak Holl, George Liu, Rong Qi, "Efficient in Vitro siRNA Delivery and Intramuscular Gene Silencing Using PEG-Modified PAMAM Dendrimers", *Mol. Pharmaceutics*, **2012**, 9, 1812-1821.
6. Yangbing Li, Zhaojun Yin, **Bo Wang**, Xiang-Bao Meng, Zhong-Jun Li, "Efficient Synthesis of Diversely Functionalized L-Hexoses from D-Glucose", *Tetrahedron*, **2012**, 68, 6981-6989.
7. **Bo Wang**, Zhaojun Yin, Yangbing Li, Ting-Xiang Yang, Xiang-Bao Meng, Zhong-Jun Li, "Active Cobalt Catalyst for the Cleavage of Benzyl Ether", *The Journal of Organic Chemistry,* **2011**, 76, 9531–9535.
8. Zhong-Jun Li, Yang-Bing Li, Zhao-Jun Yin, Shu-Chun Li, **Bo Wang**, Qin Li, Xiang-Bao Meng, *Patent*, CN 201110354102.X. Peking University, **2011**.
9. Zhao-Jun Yin, **Bo Wang**, Yang-Bing Li, Xiang-Bao Meng, and Zhong-Jun Li, "Highly Efficient and Mild Method for Regioselective De-*O*-benzylation of Saccharides by $Co_2(CO)_8$-$Et_3SiH$-CO Reagent System", *Organic Letters*, **2010**, 12, 536-539.
10. Zhong-Jun Li, Zhao-Jun Yin, Xiang-Bao Meng, Yang-Bing Li, **Bo Wang**, Qin Li, Shu-Chun Li, *Patent*, CN201010033942. 1. Peking University. July 14th, **2010**.

# Chapter 1: Introduction

## 1.1 Electrochemical Biosensors for Neurotransmitter Detection

The ability to monitor neurotransmitter release in freely behaving animals is key to understand neuronal processes underlying the progression of neurological diseases and disorders, such as Parkinson's disease. Different analytical tools are reported for monitoring neurotransmitter levels *in vivo*.

Although fast-scan cyclic voltammetry (FSCV) has proven to be an excellent electrochemical detection method, this method is only suitable for a limited number of neuromodulators individually, such as DA.[1-5] FSCV also requires specialized instrumentation and sophisticated data analysis procedures. The major excitatory neurotransmitter, glutamate (Glut), is not readily oxidized at an electrode. Microdialysis has also been used for many years for sampling of brain extracellular fluid *in vivo*, but the long analysis times (5-10 min) and relatively large probe size (≥ 200 μm) gives this tool inadequate temporal and spatial resolution.

In contrast, constant potential amperometry requires only a standard potentiostat and straightforward data collection and analysis. Amperometric electroenzymatic methods for the detection of Glut have been developed by our lab and others.[6-9] If the major electrooxidizable species are known, constant potential amperometry is the preferred electroanalytical technique. For this method, the interferents should either be excluded from the electrode surface or be below the detection limit. Oxidases are available for some major neurotransmitters such as glutamate (Glut) and choline (Ch). The oxidases selectively catalyze the oxidation of their corresponding substrate. For example, Glut oxidase (GlutOx) catalyzes the oxidative deamination of Glut in the presence of oxygen to produce α-ketoglutarate, ammonia, and hydrogen peroxide ($H_2O_2$). Therefore, this enzyme can be immobilized onto an electrode surface and the $H_2O_2$ produced may

be detected by electrooxidization to generate amperometric signals for correlation to glutamate concentration. [10-12] (**Figure 1.1**)

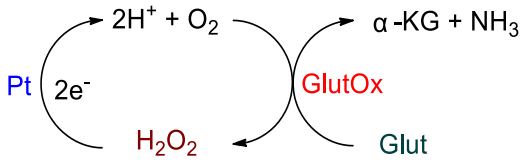


**Figure 1.1** Glutamate oxidation reaction and $H_2O_2$ electrooxidation.

Platinum (Pt) generally is used as the electrode material for electrooxidation of $H_2O_2$.[13] The efficient oxidation of $H_2O_2$ on unmodified electrodes requires a relatively high anodic potential (~0.7 V *vs.* Ag/AgCl). At this potential, electroactive neuromodulators and interferents in brain extracellular fluid such as dopamine (DA) and ascorbic acid (AA) may also be electrooxidized at the electrode surface thereby generating a current signal. Therefore, the signal from AA may mask the oxidation signal from Glut. To solve this problem, we can modify the electrode surfaces with suitable permselective polymers which could give sensor selectivity against interferents. The key point is that the surface modification should be permeable to $H_2O_2$ but not to interferents. Nafion, which is a sulfonated tetrafluoroethylene-based fluoropolymer-copolymer, is commonly used to exclude anionic interferents such as $AA^-$.[14] PPy films can be created by electropolymerizing pyrrole to repel cationic ions such as $DA^+$. [15-16] Both Nafion and PPy layers allow the permeation of small neutral molecules (e.g. $H_2O_2$). [6]

Hamdi *et al.* successfully showed that in the presence of the electroactive interferents (DA and AA), Glut is selectively detected by 125 μm diameter microbiosensors. Furthermore, the Glut sensor also exhibited a fast response time (~1 s), high selectivity and low detection limit.[7] But

oftentimes, single neurotransmitter alone does not control the complex behaviors of animals.[17-19] Therefore it is desirable to design probes capable of detecting multiple transmitters simultaneously to get a better understanding of how neurotransmitters affect an organism's behavior. The development of a flexible microelectrode array (MEA) format (**Figure 1.2**) that can contain 4 or more microelectrodes per microprobe[20-22] allows more neurochemical microbiosensors (e.g. for DA) as well as a control or reference microelectrode to be incorporated on one probe. The utility of these MEA microsensors for detection of Glut has been demonstrated in the brains of both anesthetized and freely moving rodents.[8,23-24]

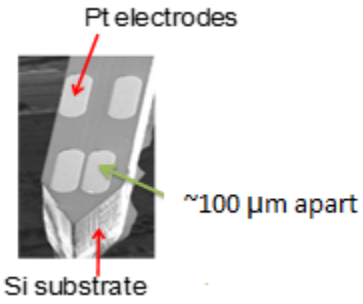


**Figure 1.2** Scanning electron microscopy (SEM) image of microelectrode array (MEA).

Fabrication of a combined Glut and DA microprobe was achieved based on a 2 × 2 MEA.[25] Each microelectrode had an average area of ~5000 $\mu m^2$. DA can be readily oxidized on Pt surface of microelectrodes. Thick PPy layer (~100 nm) on the Glut sensor site was used to repel $DA^+$. A thin overoxidized PPy layer (~1 nm) on the DA sensor site was used to improve the sensitivity of the sensor by enhancing DA adsorption at the electrode surface. Nafion layers helped repel $AA^-$. (**Figure 1.3**)

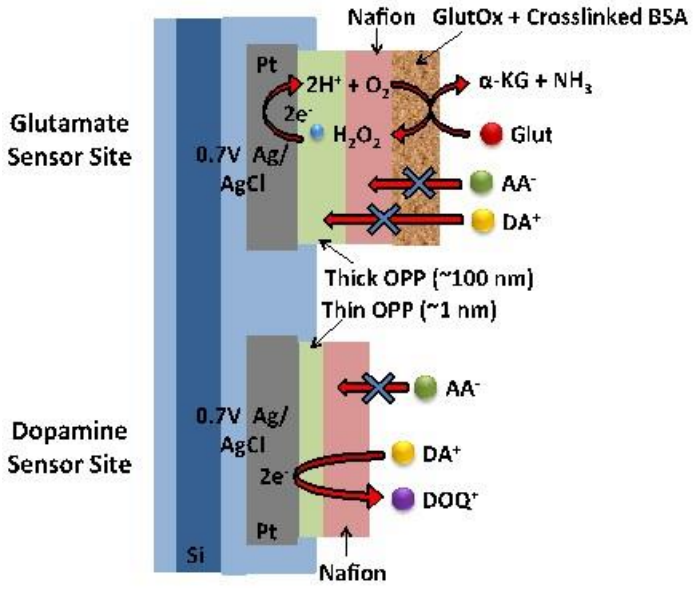


**Figure 1.3** Schematic diagram of the dual Glut/DA sensor configuration.[26]

The resulting dual Glut/DA sensor was tested *in vitro*. No responses to AA injection were observed from all sites. After injection of Glut, only Glut sensor sites gave a current response. In the presence of DA, only DA sensor site had response. The specificity of the dual Glut/DA sensing probe suggests the feasibility of combined monitoring of Glut and DA with required sensitivity and detection limit.[25] (**Figure 1.4**)

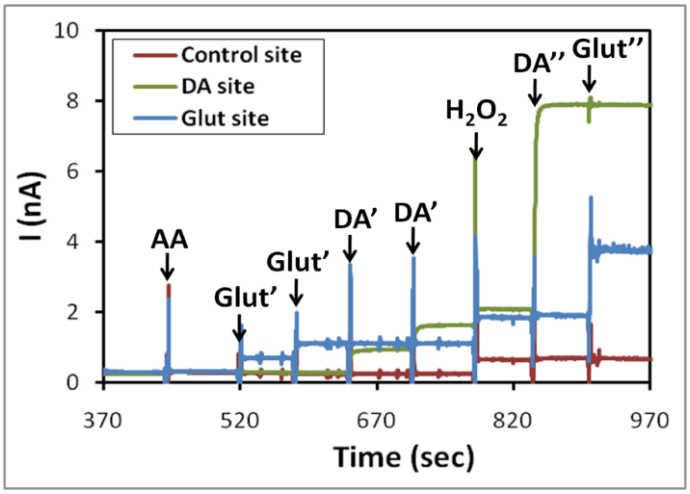

**Figure 1.4** Combined sensing of Glut and DA at a constant potential of 0.7 V (vs. Ag/AgCl). The microprobe was tested with AA, Glut, DA, $H_2O_2$, DA and Glut sequentially.

## 1.2 Enzyme immobilization

Enzyme immobilization is a key step in the biosensor fabrication process which can impact the overall biosensor performance. Common enzyme immobilization methods include crosslinking using glutaraldehyde, [27-29] enzyme entrapment in polypyrrole-derived matrices [30-31] and enzyme adsorption to the surface of the electrodes [32-33]. In the past, Tseng *et al.* used glutaraldehyde crosslinking as an enzyme immobilization method that can result in stable binding of proteins to the electrode surface.[25] During the process of cross-linking, two or more molecules are covalently bound together using glutaraldehyde, a most common crosslinking agent. Glutaraldehyde crosslinking can be performed in two widely used ways: addition of glutaraldehyde to the enzyme mixture [34] or exposure of the enzyme deposiy to saturated vapor [35]. For dual sensor fabrication (see above), the former method was used. GlutOx was immobilized to the Nafion surface by manually depositing GlutOx/BSA/glutaraldehyde crosslinking mixture.

A widely used enzyme immobilization method involves manually depositing a mixture of enzyme, BSA and GAH to selected microelectrode sites under the microscope. This method is a well-established technique to successfully construct the biosensors. However, in the case where enzyme need to be deposited on microelectrodes that are spaced less than ~100 μm apart, using manual deposition can be quite challenging. In addition, the manual enzyme deposition method may not give a uniform and consistent enzyme layer. (**Figure 1.5**)

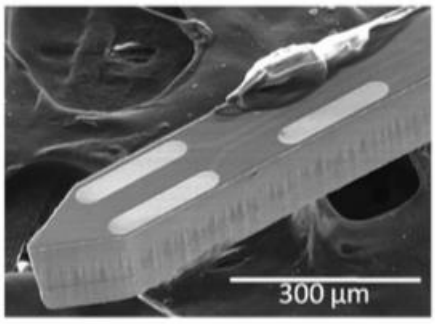


**Figure 1.5** Scanning electron microscopy (SEM) image of selective GlutOx immobilization on the top left microelectrode site previously modified with a thick OPPy film and Nafion.

In order to develop a sensor that can detect multiple neurotransmitters, there is a necessity for the development of improved, reproducible, non-manual methods for depositing enzymes selectively on microelectrodes, especially for microelectrodes less than 100 µm apart. It is even more attractive for future applications if the biosensor fabrication process is automated (non-manual).

## 1.3 Microcontact Printing (µCP)

µCP of proteins entails the transfer of layers of protein to substrates using an elastomeric stamp composed of polydimethylsilane (PDMS). The PDMS is cured at elevated temperatures (usually 60 °C) and a solid, elastomeric polymer is formed. The product contains the $–Si(CH_3)_2-O-$ structural unit.[36] Previously, this method was used by Whitesides *et al.* to find an easy and fast way to replicate patterns generated by photolithography upon introduction of µCP.[37] More recently, an elastomer, cured stamp from a mold structure was used as a tool to generate a patterned thiol self-assembled monolayers (SAMs) on the gold surface.[38-40] The stamp features are created by casting the polymer on a silicon mold that previously was micromachined through

photolithography and etching steps to give the desired features. The mechanical properties of the elastomeric PDMS stamps provide sufficient mechanical stability for the printing features down to 500 nm in size.[36]

The μCP method has also been used to directly apply patterned arrays of proteins on silicon or glass substrates. To create the stamp, a micro silicon mold is fabricated first. Next, curing liquid PDMS prepolymer is applied on the silicon mold (**Figure 1.6A**). The stamp is ready for use after peeling it off the mold. The stamps serve as a tool to transfer the enzyme onto the targeted surface. For printing of proteins, the stamp surface should be either covered with protein solution or soaked in a protein solution. After a certain equilibrium time, the inking side of the stamp is rinsed and dried. Then the stamps are used to transfer the protein "ink" to a substrate (**Figure 1.6B**). A few seconds of surface contact is sufficient, and the efficiency of transfer can exceed 99%. The transfer usually occurs only at places of contact between stamp and substrate.[41]

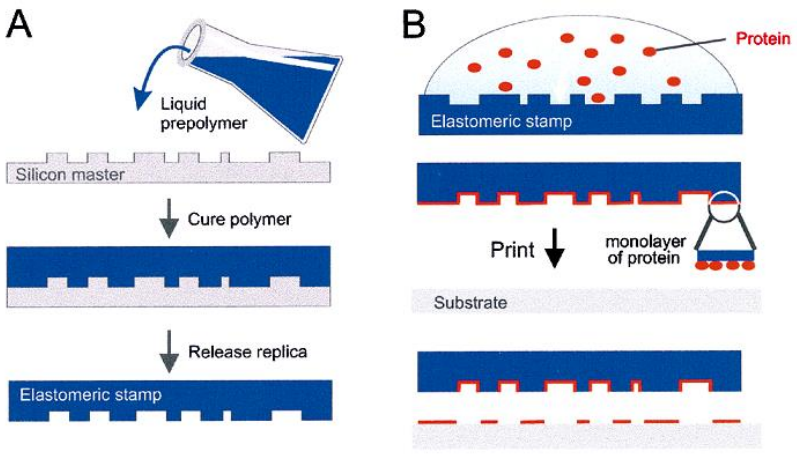


**Figure 1.6** (a) Scheme of fabrication of a stamp and (b) μCP process.[41]

Both hydrophobic and hydrophilic substrates have been used for successful transfer of protein monolayers with a resolution of ~1 μm. (e.g., see **Figure 1.7**) [41] The surface of the PDMS stamps can also be oxidized in an oxygen plasma to generate silanol group (Si-OH) on the surface.[42] This modification will form a more hydrophilic PDMS surface.

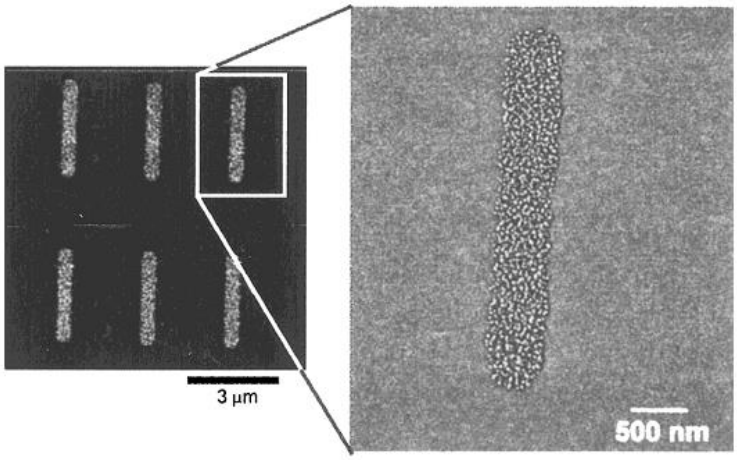


**Figure 1.7** Atomic force microscopy (AFM) images of immunoglobulins G printed onto a Si wafer.

The PDMS stamps are reusable without compromising the performance which will lower the fabrication cost. Ethanol/water (v/v=1:2) solution can be used to wash the stamps since the ethanol has a minimal swelling effect on the polymer.[43] Hiroshi Matsui *et al.*[44] previously demonstrated that the direct stamping of urease enables the simultaneous patterning and covalent cross-linking of urease by modifying the substrate to display aldehyde groups. Furthermore, reduced enzyme deactivation was observed compared to glutaraldehyde crosslinking in solution. Above all, μCP is an effective method that can potentially provide consistent results and defined pattern printing.

## 1.4 Chitosan Deposition

To further improve the enzyme transfer process, it may prove beneficial to combine the chitosan electrodeposition step with enzyme deposition by microcontact printing (μCP). Chitosan is a polysaccharide and it has some unique properties that can be used in electrochemical deposition methods for providing selective and efficient enzyme immobilization.[45] The change of pH can alter the charge state of the chitosan. Negative potential will cause deprotonation of amine groups on chitosan resulting in its precipitation on an electrode surface.[46-47]

Very recently, Tseng *et al.* demonstrated the use of electrodeposited chitosan to direct the adsorption of glutamate oxidase on selected microelectrodes so as to fabricate glutamate microbiosensors.[48] In this method, enzyme is adsorbed to chitosan layers that have been coated on the microelectrode surface. First, chitosan is selectively deposited by simply applying a negative potential on the desired site producing a uniform deposition area as a result of an increase of the local pH.[45] The microelectrodes are then immersed in GlutOx solution overnight for enzyme adsorption. This enzyme immobilization method is simple and selective. However, compared to sensor prepared using a manual coating process, the Glut sensor generated by this method had a lower sensitivity.[25] This decreased sensitivity may be a result of a lower immobilized GlutOx concentration on the chitosan surface as well as non-covalent surface attachment.

## 1.5 Electrochemical Impedance Spectroscopy

To monitor the progress of enzyme layer deposition, electrochemical impedance spectroscopy (EIS) can be used to report the impedance change of the electrode surface.[49-55] In

EIS, the impedance of a system can be determined by applying a voltage perturbation with a small amplitude and then detecting the current response using a ferri-/ferrocyanide probe. As the surface modification continues, different impedances will be observed. A good example can be seen from the glucose sensor fabrication by Biru Hu *et al.* (**Figure 1.8**)[55] Nyquist plots (-Z'' *vs.* Z') of electrodes at different modification steps were shown below. During the process of modification, significant differences in the impedance spectra were observed. The diameter of the respective semicircular element corresponds to the electron transfer resistance at the electrode surface. The diameter increased as layers of glucose oxidase (GOx) on the electrode increased.

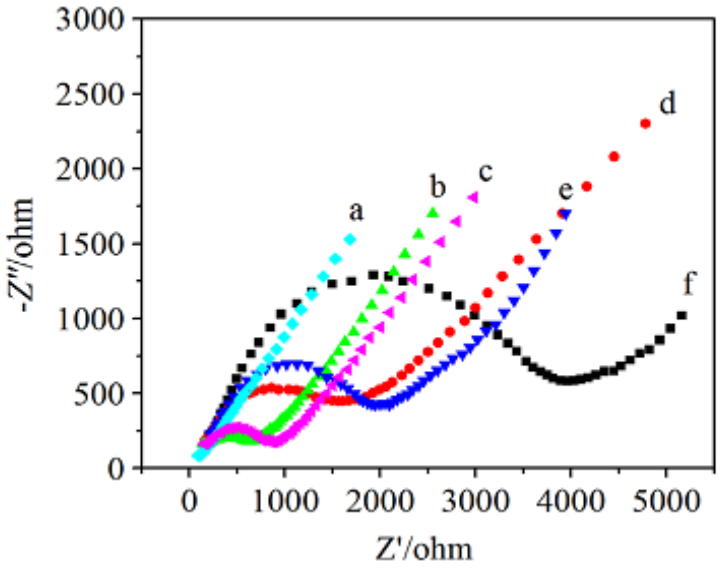


**Figure 1.8** EIS for the cysteamine modified Au electrode with different numbers of glucose oxidase in 5 mM $K_3Fe(CN)_6/K_4Fe(CN)_6$ (molar ratio is 1:1) solution. (a) Au/cysteamine; (b) Au/cysteamine/GOx and Au/cysteamine/GOx/chitosan; (c)–(f) with different layers of G.[55]

## 1.6 Platinum Black and Platinum Nanograss

As mentioned above, Platinum (Pt) generally is used as the electrode material for electrooxidation of $H_2O_2$ at a relatively high anodic potential (~0.7 V *vs.* Ag/AgCl).[13] However, a great drawback of this method is high potential used for $H_2O_2$ oxidation. Many electroactive interferences in real sample (such as ascorbic acid (AA) *etc.*) could be oxidized to cause false signals. Besides coating permselective polymer layers, several alternative approaches have been employed to lower the oxidation potential of $H_2O_2$, such as using horseradish peroxidase or redox mediators.[56-59]

In addition, some surface modification materials (such as Pt black) could be used to enlarge the surface area resulting in potential reduction.[7] Pt black is often used for this purpose due to its simple manipulation. Pt black, which is a "spongy" electrodeposit of platinum, has been shown to be one of the best electrode materials for oxidation of $H_2O_2$.[60] Hamdi *et al.* reported a glutamate microbiosensor consisting of Pt black electrodeposited Pt wire working at a reduced potential (0.45 V *vs.* Ag/AgCl).[7]

However, practical applicability of Pt black is limited as a consequence of its low mechanical stability.[61-63] In addition, the Pt black coating solution often includes 0.01% lead acetate[64] and has been reported to cause cytotoxic reaction if traces of lead used in the electrolyte during fabrication, elute from the final coating *in vivo*.[65] Recently, Boehler *et al.* introduced a nanostructured Pt-coating as an add-on functionalization for impedance reduction of small electrodes.[66] In comparison to Pt black deposition, all chemicals used in the deposition process are non-cytotoxic. The grass-like nanostructure was found to reduce the impedance by almost two orders of magnitude compared to untreated samples. The Pt-grass coating method is performed via a simple electrochemical process which can be applied to virtually any electrode type and

accordingly shows potential as a universal impedance reduction strategy. Their elution tests revealed non-toxicity of the Pt-grass and the coating was found to exhibit strong adhesion to the metallized substrate.

## 1.7 References


[1] Maidment, N. T.; Marsden, C. A. Neuropharmacology 26 (1987) 187-193.

[2] Maidment, N. T.; Marsden, C. A. Eur J Pharmacol 136 (1987) 141-149.

[3] Maidment, N. T.; Marsden, C. A. Brain Res 338 (1985) 317-325.

[4] Crespi, F.; Sharp, T.; Maidment, N. T.; Marsden, C. A. Brain Res 322 (1984) 135-138.

[5] Crespi, F.; Sharp, T.; Maidment, N.; Marsden, C. Neurosci Lett 43 (1983) 203-207.

[6] Hamdi, N.; Wang, J. J.; Monbouquette, H. G. J Electroanal Chem 581 (2005) 258-264.

[7] Hamdi, N.; Wang, J. J.; Walker, E.; Maidment, N. T.; Monbouquette, H. G. J Electroanal Chem 591 (2006) 33-40.

[8] Walker, E.; Wang, J.; Hamdi, N.; Monbouquette, H. G.; Maidment, N. T. Analyst 132 (2007) 1107-1111.

[9] Burmeister, J. J.; Pomerleau, F.; Palmer, M.; Day, B. K.; Huettl, P.; Gerhardt, G. A. J Neurosci Methods 119 (2002) 163-171.

[10] Cosnier, S.; Innocent, C.; Allien, L.; Poitry, S.; Tsacopoulos, M. Anal Chem 69 (1997) 968-971.

[11] Mulchandani, A.; Wang, C. L. Electroanal 8 (1996) 414-419.

[12] White, S. F.; Turner, A. P. F.; Bilitewski, U.; Schmid, R. D.; Bradley, J. Anal Chim Acta 295 (1994) 243-251.

[13] O'Neill, R. D.; Chang, S. C.; Lowry, J. P.; McNeil, C. J. Biosens Bioelectron 19 (2004) 1521-1528.

[14] Gerhardt, G. A.; Oke, A. F.; Nagy, G.; Moghaddam, B.; Adams, R. N. Brain Res 290 (1984) 390-395.

[15] Hsueh, C. C.; Brajtertoth, A. Anal Chem 66 (1994) 2458-2464.

[16] Pihel, K.; Walker, Q. D.; Wightman, R. M. Anal Chem 68 (1996) 2084-2089.

[17] Andre, V. M.; Cepeda, C.; Cummings, D. M.; Jocoy, E. L.; Fisher, Y. E.; Yang, X. W.; Levine, M. S. Eur J Neurosci 31 (2010) 14-28.

[18] Andre, V. M.; Cepeda, C.; Levine, M. S. Cns Neuroscience & Therapeutics 16 (2010) 163-178.

[19] Cepeda, C.; Andre, V. M.; Yamazaki, I.; Wu, N. P.; Kleiman-Weiner, M.; Levine, M. S. Eur J Neurosci 27 (2008) 671-682.

[20] Konradsson-Geuken, A.; Gash, C. R.; Alexander, K.; Pomerleau, F.; Huettl, P.; Gerhardt, G. A.; Bruno, J. P. Synapse 63 (2009) 1069-1082.

[21] Mattinson, C. E.; Burmeister, J. J.; Quintero, J. E.; Pomerleau, F.; Huettl, P.; Gerhardt, G. A. J Neurosci Methods 202 (2011) 199-208.

[22] Parikh, V.; Pomerleau, F.; Huettl, P.; Gerhardt, G. A.; Sarter, M.; Bruno, J. P. Eur J Neurosci 20 (2004) 1545-1554.

[23] Wassum, K. M.; Tolosa, V. M.; Tseng, T. C.; Balleine, B. W.; Monbouquette, H. G.; Maidment, N. T. J Neurosci 32 (2012) 2734-2746.

[24] Wassum, K. M.; Tolosa, V. M.; Wang, J. J.; Walker, E.; Monbouquette, H. G.; Maidment, N. T. Sensors 8 (2008) 5023-5036.

[25] Tseng, T. T. C.; Monbouquette, H. G. J Electroanal Chem 682 (2012) 141-146.

[26] Tseng, T. T.; Monbouquette, H. G. J Electroanal Chem (Lausanne Switz) 682 (2012) 141-146.

[27] Burmeister, J. J.; Moxon, K.; Gerhardt, G. A. Anal Chem 72 (2000) 187-192.

[28] Strike, D. J.; Derooij, N. F.; Koudelkahep, M. Sensor Actuat B-chem 13 (1993) 61-64.

[29] Wilson, R.; Turner, A. P. F. Biosens Bioelectron 7 (1992) 165-185.

[30] McMahon, C. P.; Killoran, S. J.; O'Neill, R. D. J Electroanal Chem 580 (2005) 193-202.

[31] Tian, F. M.; Gourine, A. V.; Huckstepp, R. T. R.; Dale, N. Anal Chim Acta 645 (2009) 86-91.

[32] Okahata, Y.; Tsuruta, T.; Ijiro, K.; Ariga, K. Thin Solid Films 180 (1989) 65-72.

[33] Singhal, R.; Takashima, W.; Kaneto, K.; Samanta, S. B.; Annapoorni, S.; Malhotra, B. D. Sensor Actuat B-chem 86 (2002) 42-48.

[34] Hu, Y. B.; Mitchell, K. M.; Albahadily, F. N.; Michaelis, E. K.; Wilson, G. S. Brain Res 659 (1994) 117-125.

[35] Pernot, P.; Mothet, J. P.; Schuvailo, O.; Soldatkin, A.; Pollegioni, L.; Pilone, M.; Adeline, M. T.; Cespuglio, R.; Marinesco, S. Anal Chem 80 (2008) 1589-1597.

[36] Torres, C. M. S. Kluwer Academic/ Plenum Publishers, New York (2003).

[37] Wallraff, G. M.; Hinsberg, W. D. Chem Rev 99 (1999) 1801-1821.

[38] Kumar, A.; Biebuyck, H. A.; Whitesides, G. M. Langmuir 10 (1994) 1498-1511.

[39] Kumar, A.; Whitesides, G. M. Appl Phys Lett 63 (1993) 2002-2004.

[40] Wilbur, J. L.; Kumar, A.; Biebuyck, H. A.; Kim, E.; Whitesides, G. M. Nanotechnology 7 (1996) 452-457.

[41] Bernard, A.; Delamarche, E.; Schmid, H.; Michel, B.; Bosshard, H. R.; Biebuyck, H. Langmuir 14 (1998) 2225-2229.

[42] Qin, D.; Xia, Y.; Whitesides, G. M. Nat Protoc 5 (2010) 491-502.

[43] Younan Xia. Milan Mrksich, E. K., and George M. Whitesides J Am Chem Soc 117 (1995) 9576-9577

[44] Fabijanic, K. I.; Perez-Castillejos, R.; Matsui, H. J Mater Chem 21 (2011) 16877.

[45] Yi, H. M.; Wu, L. Q.; Bentley, W. E.; Ghodssi, R.; Rubloff, G. W.; Culver, J. N.; Payne, G. F. Biomacromolecules 6 (2005) 2881-2894.

[46] Wu, L. Q.; Gadre, A. P.; Yi, H. M.; Kastantin, M. J.; Rubloff, G. W.; Bentley, W. E.; Payne, G. F.; Ghodssi, R. Langmuir 18 (2002) 8620-8625.

[47] Koev, S. T.; Dykstra, P. H.; Luo, X.; Rubloff, G. W.; Bentley, W. E.; Payne, G. F.; Ghodssi, R. Lab on a Chip 10 (2010) 3026-3042.

[48] Tseng, T. T. C.; Yao, J.; Chan, W. C. Biochem Eng J 78 (2013) 146-153.

[49] Hou, Y.; Helali, S.; Zhang, A.; Jaffrezic-Renault, N.; Martelet, C.; Minic, J.; Gorojankina, T.; Persuy, M. A.; Pajot-Augy, E.; Salesse, R.; Bessueille, F.; Samitier, J.; Errachid, A.; Akimov, V.; Reggiani, L.; Pennetta, C.; Alfinito, E. Biosens Bioelectron 21 (2006) 1393-1402.

[50] Lisdat, F.; Schafer, D. Anal Bioanal Chem 391 (2008) 1555-1567.

[51] Nowicka, A. M.; Fau, M.; Rapecki, T.; Donten, M. Electrochim Acta 140 (2014) 65-71.

[52] Pruneanu, S.; Pogacean, F.; Biris, A. R.; Ardelean, S.; Canpean, V.; Blanita, G.; Dervishi, E.; Biris, A. S. The Journal of Physical Chemistry C 115 (2011) 23387-23394.

[53] Wang, M.; Wang, L.; Wang, G.; Ji, X.; Bai, Y.; Li, T.; Gong, S.; Li, J. Biosensors and Bioelectronics 19 (2004) 575-582.

[54] Yousef Elahi, M.; Khodadadi, A. A.; Mortazavi, Y. J Electrochem Soc 161 (2014) B81-B87.

[55] Zhang, Y.; Li, Y.; Wu, W.; Jiang, Y.; Hu, B. Biosens Bioelectron 60 (2014) 271-276.

[56] Dicks, J. M.; Hattori, S.; Karube, I.; Turner, A. P. F.; Yokozawa, T. Ann Biol Clin-paris 47 (1989) 607-619.

[57] Kulagina, N. V.; Shankar, L.; Michael, A. C. Anal Chem 71 (1999) 5093-5100.

[58] Bartlett, P. N.; Ali, Z.; Eastwickfield, V. Journal of the Chemical Society-Faraday Transactions 88 (1992) 2677-2683.

[59] Iwakura, C.; Kajiya, Y.; Yoneyama, H. Journal of the Chemical Society-Chemical Communications (1988) 1019-1020.

[60] Khan, G. F.; Wernet, W. J Electrochem Soc 143 (1996) 3336-3342.

[61] ROBINSON, D. A. P IEEE 56 (1968) 1065-1071.

[62] Sharanya Arcot Desai, J. D. R., Liang Guo, and Steve M. Potter Front Neuroengineering 3 (2010) 1-5.

[63] Tang, R. Y.; Pei, W. H.; Chen, S. Y.; Zhao, H.; Chen, Y. F.; Han, Y.; Wang, C. L.; Chen, H. D. Science China-Information Sciences 57 (2014).

[64] Maher, M. P.; Pine, J.; Wright, J.; Tai, Y. C. J Neurosci Meth 87 (1999) 45-56.

[65] Schuettler M, D. T., Wien SL, Becker S, Staiger A, Hanauer M, Kammer S, Stieglitz T 10th Annual Conference of the International FES Society, Montreal, Canada (2005).

[66] Boehler, C.; Stieglitz, T.; Asplund, M. Biomaterials 67 (2015) 346-353.

# Chapter 2: Enzyme Deposition by Polydimethylsiloxane Stamping for Biosensor Fabrication

## 2.1 Abstract

High-performance biosensors were fabricated by efficiently transferring enzyme onto electrode surfaces using a polydimethylsiloxane (PDMS) stamp. The stamping method was pursued as an effective means to transfer enzyme to a modified Pt electrode surface in high concentration layers so as to achieve both rapid response time and high sensitivity. Polypyrrole and Nafion were coated first on the electrode surface to act as permselective films for exclusion of both anionic and cationic electrooxidizable interferents (*e.g.*, ascorbic acid and dopamine) found in brain extracellular fluid. A chitosan film then was electrochemically deposited to serve as an adhesive layer for enzyme immobilization. Glucose oxidase (GOx) was selected as a model enzyme for construction of a glucose biosensor, and a mixture of GOx and bovine serum albumin (BSA) was stamped onto the chitosan-coated surface and subsequently crosslinked using glutaraldehyde vapor. The biosensor fabrication process was monitored by electrochemical impedance spectroscopy, and the electrode surface before and after GOx/BSA stamping was examined by scanning electron microscopy. For the optimized fabrication process, the biosensor exhibited excellent performance characteristics including a linear range up to 2 mM with sensitivity of 29.4 ± 1.3 μA $mM^{-1}$ $cm^{-2}$ and detection limit of 4.3 ± 1.7 μM (S/N = 3) as well as a rapid response time of ~2 s. In comparison to those previously described, this glucose biosensor exhibits an excellent combination of high sensitivity, low detection limit, rapid response time, and good selectivity. Thus, these results support the use of PDMS stamping as an effective enzyme deposition method for electroenzymatic biosensor fabrication, which may prove especially useful

for the high throughput deposition of enzyme at selected sites on microelectrode array microprobes of the kind used for neuroscience research *in vivo*.

## 2.2 Introduction

Electroenzymatic biosensors utilize an enzyme as the biological recognition element, which is coupled to an electrode that serves as a transducer to convert the recognition event into a measurable signal. Typically, the means by which the enzyme is deposited and immobilized on the electrode surface constitute the critical steps in biosensor fabrication, as the immobilized enzyme concentration and activity directly impact sensor performance. Many approaches have been taken in an effort to deposit enzyme in an active state on the electrode surface including drop coating, layer-by-layer assembly, adsorption, and electrodeposition [1-6]. Commercially available glucose sensors for home blood glucose monitoring commonly are fabricated by screen-printing [7], which typically has a resolution of 50-150 μm [8]. However, we ultimately are searching for a simple technique enabling the simultaneous transfer of enzyme at high concentration to multiple preselected sites on our microelectrode array microprobes with micron-scale resolution for neurochemical sensing applications *in vivo* [9].

Tseng *et al.* recently demonstrated the use of electrodeposited chitosan to direct the adsorption of glutamate oxidase (GlutOx) on selected microelectrodes so as to fabricate glutamate microbiosensors [10-11]. Chitosan may be deposited selectively on microelectrodes at negative potential, as the high local pH in the vicinity of the electrodes results in the deprotonation of amine groups on chitosan resulting in its precipitation [12-13]. These amine groups on the electrodeposited chitosan attract typically negatively charged proteins for adsorption and are available for subsequent crosslinking. However, simple adsorption of GlutOx on the chitosan film

resulted in a less active, presumably lower concentration deposit than that obtained by manual deposition, which was reflected in a lower performance glutamate sensor.

In recent years, polydimethylsiloxane (PDMS) stamps have been employed to transfer protein in a micron to submicron-resolution pattern to various substrates in a process referred to as microcontact printing [14-20]. The mechanical properties of the PDMS stamps provide sufficient mechanical stability for printing features as small as 500 nm [15]. Importantly, many proteins retain their biological activity after printing, and the transfer of proteins can occur in a few seconds [16]. In addition, the stamp often does not pick up protein already printed. Thus, the PDMS stamping process has been regarded as a unidirectional process for protein transfer. After protein deposition, the PDMS stamps can be washed and reused. Therefore, we hypothesized that the PDMS stamping process may be an excellent, high-resolution method for transferring concentrated enzyme onto arrays of Pt microelectrodes on micromachined silicon microprobes. Such microprobes were used by our collaborators to monitor neurotransmitter release in the brains of freely moving laboratory rats [9,21].

In this study, the transfer of glucose oxidase (GOx) to modified Pt electrode surfaces was employed as a model system to demonstrate, for the first time, the utility of the PDMS stamping method for creation of high-performance (*e.g.*, high sensitivity, low detection limit, excellent selectivity and fast response time), electroenzymatic biosensors. In these biosensors, the immobilized GOx catalyzes the oxidation of glucose to D-glucono-1,5-lactone with concomitant production of hydrogen peroxide. The underlying electrode, held at positive potential, electrooxidizes the hydrogen peroxide giving rise to a measurable Faradaic current. Sensor selectivity against common interferents is achieved by modifying the electrode surface with permselective polymers such as Nafion and polypyrrole. Thicker polypyrrole films exclude both

cations and anions and Nafion rejects anionic interferents [2,22]. Glucose biosensors obviously are useful for a variety of applications both *in vitro* and *in vivo*. Based on recent comprehensive reviews, home use blood glucose biosensors have been the most successful biosensor products to date by a wide margin, and amperometric glucose biosensors based on immobilized GOx or glucose dehydrogenase are the most common. The typical test range of these commercial glucose biosensors is ~0.6 mM-33.3 mM and the reported assay time varies from 5 to 20 s [7,23]. However, our interest is in sensors useful for neuroscience research *in vivo*, thus the emphasis on response time, sensitivity (so that sensors may be miniaturized) and rejection of dopamine and ascorbic acid, which are electrooxidizable interferents common to brain extracellular fluid.

## 2.3 Material and methods

### *2.3.1 Reagents*

Glucose oxidase (from *Aspergillus niger*, CAS NO. 9001-37-0), pyrrole (Py), Nafion® (5%), glutaraldehyde solution (25%), bovine serum albumin (BSA) lyophilized powder, hydrogen peroxide solution (30%), chitosan (From crab shells, minimum 85% deacetylated), D-(+)-glucose, L-ascorbic acid, dopamine hydrochloride, potassium hexacyanoferrate (II) trihydrate, and potassium hexacyanoferrate (III) were purchased from Sigma-Aldrich (St. Louis, MO). Isopropyl alcohol and 1M sulfuric acid solutions were obtained from Fisher Scientific (Pittsburgh, PA). Ag/AgCl glass-bodied reference electrodes with 3 M NaCl electrolyte, 0.5-mm-diameter Pt wire auxiliary electrodes and disk Pt electrodes (1.6 mm dia.) were purchased from BASi (West Lafayette, IN). Sodium phosphate buffer (PBS, pH 7.4) was composed of 50 mM sodium phosphate (dibasic) and 100 mM sodium chloride. Microcloth (PSA, 2-7/8'') for electrode polishing was purchased from Buehler, An ITW Company (Lake Bluff, Illinois). Ultrapure water

was generated using a Millipore Milli-Q Water System and was used for preparation of all solutions.

### *2.3.2 Instrumentation*

Electrochemical experiments for sensor development, evaluation and calibration were performed using a Versatile Multichannel Potentiostat (model VMP3) equipped with the 'p' low current option and N'Stat box driven by EC-LAB software (Bio-Logic USA, LLC, Knoxville, TN) in a three electrode configuration consisting of the sensing electrode, a Pt wire auxiliary electrode, and a Ag/AgCl glass-bodied reference electrode. A Nova Nano 230 was used for environmental SEM images. An Infinit® M1000 PRO was used for fluorescence assays.

### *2.3.3 Fabrication of polydimethylsiloxane stamps*

Polydimethylsiloxane (PDMS) stamps were fabricated using the Sylgard® 184 silicone elastomer kit from Dow Corning. The curing agent and monomer were mixed at a 1:10 ratio in a Petri Dish to give a ~2-mm-thick polymer film. Subsequently, the mixture was carefully degassed under vacuum and cured at 60 ℃ for 4 hrs. A cylindrical feature of ~1.6 mm diameter and ~2 mm height was punched from the film and a rectangular PDMS support (~5 mm square) was cut as well. Next, the cylindrical PDMS piece was glued at the center of the rectangular piece using an uncured mixture of curing agent and base monomer. The assembled PDMS stamp was ready after curing at 60 ℃ for 4 hours. The PDMS stamps were washed with ethanol/water (v/v = 1:2) and reused [20].

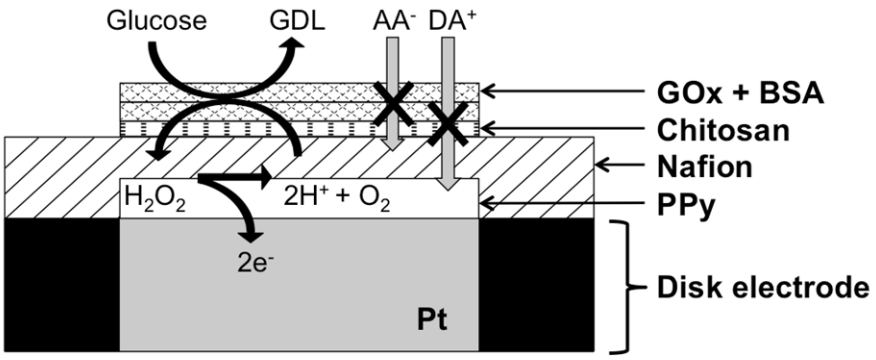


**Figure 2.1** Schematic diagram of the glucose sensor configuration (not to scale). Ascorbic acid and dopamine are rejected primarily by Nafion and PPy, respectively.

### *2.3.4 Sensor preparation*

The sensor was prepared layer-by-layer to achieve the final configuration illustrated in **Figure 2.1.** The Pt disk electrode (1.6 mm dia.) was polished using a microcloth with a 0.05 μm particle suspension. After rinsing with ultrapure water, it was sonicated in isopropyl alcohol followed by electrochemical cleaning with 0.5 M sulfuric acid and ultrapure water, respectively. Next, a polypyrrole (PPy) film was electrodeposited (200 mM Py in stirred PBS, 0.85 V *vs.* Ag/AgCl, ~5 min) onto the Pt surface, followed by Nafion dip-coating twice with a 5% Nafion® solution and baking in an oven at 180 ℃ for 3 min [2,22,24].

The pH of the chitosan solution (0.04% m/v) was adjusted to pH 3 using hydrochloric acid (HCl) to dissolve the chitosan flakes. After filtering with a 0.2 μm syringe filter, the pH was adjusted to 5 using sodium hydroxide (NaOH) solution (0.5 M). A constant potential of -0.7 V *vs.* Ag/AgCl was applied at the PPy/Nafion-coated Pt electrode surface for 2 min while immersed in

the chitosan solution to electrodeposit a chitosan film [10,13]. This chitosan-coating process was repeated two more times.

A droplet of GOx/BSA solution, mixed in a 1:1 mass ratio (BSA: 10 mg/mL; GOx 10 mg/mL) in PBS, was placed on the cleaned PDMS stamp surface and left at room temperature for ~10 min (inking time). The excess protein solution was carefully wicked from the stamp with a Kimwipe, and the stamp was dried under a stream of argon for ~30 s. The stamp then was placed horizontally in contact with the chitosan-coated electrode surface for 10-15 s. Subsequently, the disk electrode surface was exposed to the vapor from a 12.5% GAH solution at room temperature for 10 s to 10 min. If the sensor was treated with multiple layers of stamped protein, each layer was treated with GAH vapor prior to stamping of the next layer. Chitosan was deposited only before the first enzyme layer transfer. Finally, the sensors were washed with ultrapure water and kept at 4 ℃ under dry conditions when not in use.

### *2.3.5 Electrochemical measurements*

Constant potential amperometric measurements were conducted in PBS buffer at 0.7 V *vs.* Ag/AgCl and at ambient laboratory temperature. More than 30 min of equilibrium time in PBS buffer was required to achieve a stable current before adding analytes. Faradaic impedance measurements were performed in the presence of $K_3Fe(CN)_6/K_4Fe(CN)_6$ (1:1)-mixture as a redox probe in PBS, using an AC voltage amplitude of 5 mV. Impedance measurements were performed at a bias potential of 0.2 V *vs.* Ag/AgCl over a frequency range from 0.1 to 1 x $10^5$ Hz [1,25].

### *2.3.6 Quantification of immobilized glucose oxidase*

To estimate the thickness of the enzyme layer and enzyme concentration on the electrode surface, a fluorescence assay was implemented using an Infinit® M1000 PRO microplate reader. The two fluorescent FAD moieties per GOx protein enable measurement of GOx concentration as

FAD fluorescence using a method developed by Gooding *et al*. [5,26]. A calibration curve was created from recordings of the fluorescence intensity of various concentrations of FAD in an aqueous solution of 8 M urea and 0.05 M KCl. The FAD solutions were stored in the dark until use. The emission intensity at 525 nm scaled linearly with the FAD concentration between 19.2 nM and 1229.7 nM at an excitation wavelength of 375 nm. Enzyme-coated electrodes were soaked in 0.7 mL of 8 M urea solution overnight to ensure that FAD was leached completely from the electrode surface. The emission intensity at 525 nm was then measured and correlated to enzyme concentration using the calibration curve described above.

## 2.4 Results and discussion

### *2.4.1 Biosensor surface morphology*

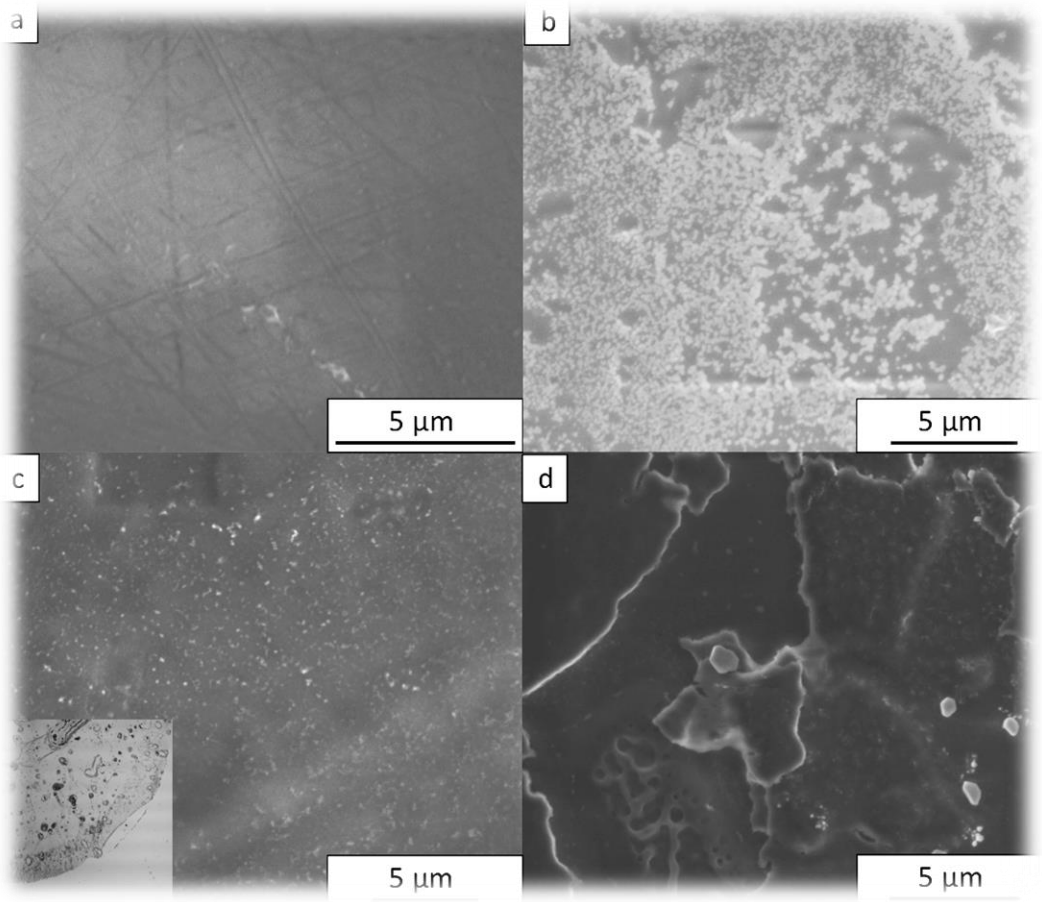


**Figure 2.2** Scanning electron microscopic (SEM) images of (a) Pt/PPy/Nafion, (b) Pt/PPy/Nafion/Chitosan, (c) Pt/PPy/Nafion/Chitosan/GOx-BSA (Inset: 50× light microscope image of stamped GOx-BSA on a Pt surface showing the edge of the stamped area) and (d) Pt/PPy/Nafion/Chitosan/GOx-BSA/GOx-BSA.

The surface morphology of each layer of the glucose biosensor was examined using environmental SEM (**Figure 2.2**). The dip-coated, Nafion film was smooth without noticeable

structure at the magnification used **Figure 2.2a**. The lines shown in **Figure 2.2a** reflected scratches on the underlying platinum disk electrode. Previously reported SEM images of electrodeposited chitosan [1] showed a sponge-like structure, however, the chitosan surface shown in **Figure 2.2b** appears to consist of a somewhat non-uniform assembly of small particles. This difference likely is due to the fact that in this work, the chitosan solution was filtered through a 0.2-μm-pore membrane immediately before use. In contrast, after two days, the chitosan likely aggregated causing relatively large particles to be deposited.

The first GOx-BSA film stamped on the chitosan layer was quite uniform (**Figure 2.2c**) despite some inconsistency in the underlying chitosan layer, however the second stamped layer of GOx-BSA appeared to be incomplete (**Figure 2.2d**). This difference in stamping efficiency between the two layers may be indicative of the importance of the chitosan film in providing an adhesive layer for the GOx-BSA deposit [10-12].

### *2.4.2 Electrochemical impedance spectroscopy (EIS)*

The fabrication process for the glucose biosensor was monitored by EIS and demonstrated that each layering step resulted in an expected change in impedance [1,25,27]. **Figure 2.3** shows the impedance features as Nyquist plots (-Im(Z) vs. Re(Z)) during the electrode modification process. The Nyquist plot consists of two regimes; a semicircular part at high frequency reflecting electron transfer resistance ($R_{ct}$) and a linear part at low frequency corresponding to a diffusion-limited process. The spectrum for the PPy modified electrode consisted of an almost straight line (**Figure 2.3a**) without a noticeable semicircular regime due to the fact that the thin PPy layer on an electrode acts primarily as a diffusional resistance. However as more insulating layers are added, the diameter of the semicircular regime increases as expected. **Figure 2.3b** is the spectrum after Nafion and chitosan films were added to the Pt/PPy electrode, and **Figs. 2.3c-e** show

significant differences in resistance after the addition of each of three protein layers by PDMS stamping.

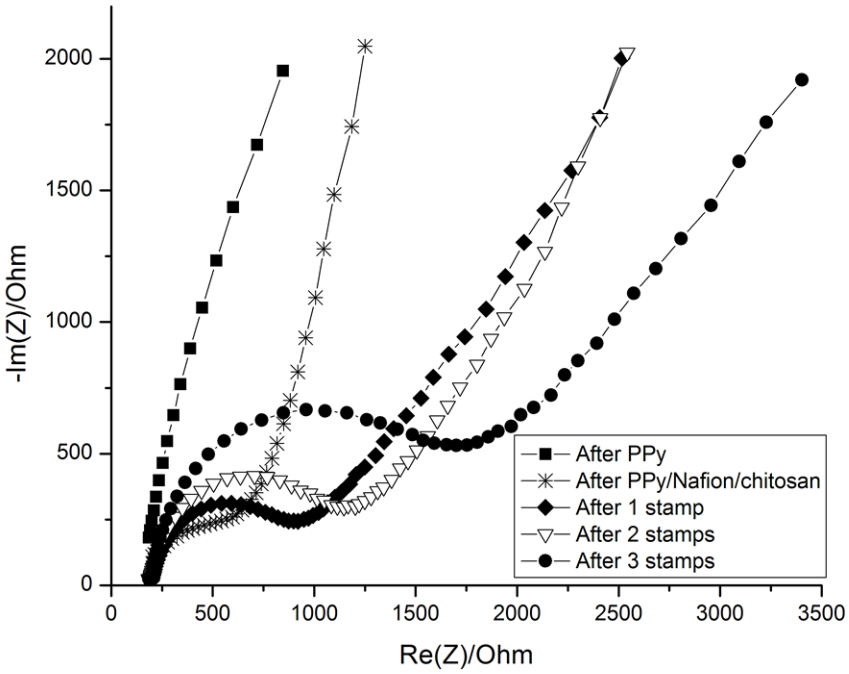


**Figure 2.3** Electrochemical impedance spectra for the modified Pt electrode at sequential steps in preparation of the glucose biosensor in 5 mM $K_3Fe(CN)_6/K_4Fe(CN)_6$ (1:1 molar ratio) in PBS solution. (a) Pt/PPy; (b) Pt/PPy/Nafion/chitosan; (c)-(e) with successive layers of GOx/BSA protein ((c) one layer; (d) two layers; (e) three layers.)

### *2.4.3 Effect of interferents*

The glucose biosensor selectivity was tested with ascorbic acid and dopamine, common electrooxidizable interferents in brain extracellular fluid. Physiologically relevant concentrations of 5 and 10 μM dopamine and 250 and 500 μM ascorbic acid were used, and a negligible biosensor

response was observed at the constant operating potential of 0.7 V (*vs.* Ag/AgCl) (**Figure 2.4**), although the representative biosensor shown exhibited the expected response to glucose and hydrogen peroxide. This result shows that polypyrrole and Nafion block access of these key electroactive interferents, which suggests that the biosensor may be useful for neuroscience research *in vivo*. In order to achieve the selectivity shown, the applied potential for chitosan deposition atop the permselective polymer coatings was set at -0.7 V, which is sufficient to create a high local pH for chitosan precipitation on the electrode surface without disrupting the underlying PPy and Nafion films [10,13].

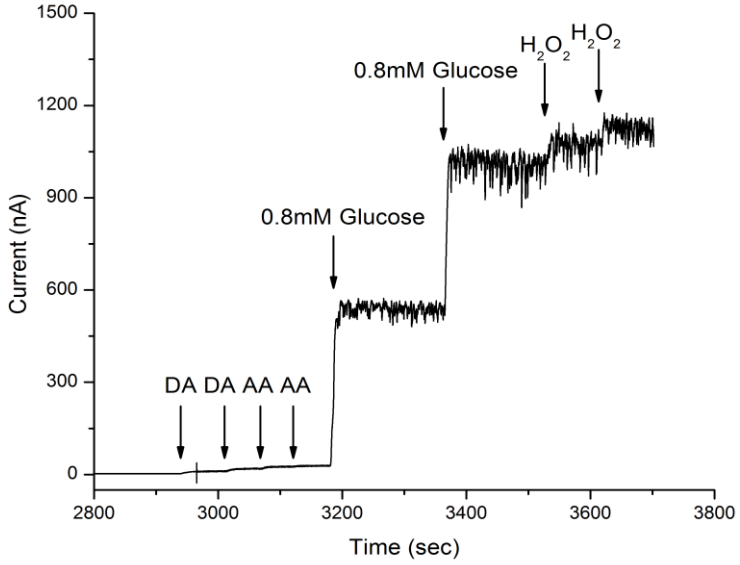


**Figure 2.4** Current responses of the glucose biosensor to interferents, glucose, and $H_2O_2$. The biosensor response at a constant potential of 0.7 V (vs. Ag/AgCl) was monitored in stirred PBS solution upon sequential injections to give 5 and 10 μM of dopamine (DA), followed by 250 and 500 μM of ascorbic acid (AA), 0.8 and 1.6 mM of glucose (Glu), and 20 μM and 40 μM of hydrogen peroxide ($H_2O_2$).

### *2.4.4 GOx deposition by PDMS stamping*

After a droplet of GOx and BSA mixture (1:1 mass ratio) was placed onto the PDMS stamp surface for ~10 min, the excess solution was removed and the stamp surface was dried. GOx and BSA on the PDMS stamp surface were transferred to the modified electrode surface by stamping for 10-15 seconds. A smooth electrode surface likely facilitated the enzyme transfer due to uniform surface contact, and filtration of the chitosan solution before electro-deposition likely helped to generate the smooth chitosan deposit (see **Figure 2.1** for surface morphology of the chitosan deposit).

The stamped enzyme layers were stabilized by exposure to saturated glutaraldehyde vapor for cross-linking. A short exposure time (*i.e.*, <30 s) resulted in an unstable protein layer that was washed away easily, while a long exposure time (*i.e.*, >5 min) resulted in unacceptable loss in enzyme activity. In addition, one layer of stamped enzyme was found to give unsatisfactory sensor performance, while three layers of enzyme commonly resulted in a long biosensor response time (*i.e.*, >3 s). Finally, the exposure time to glutaraldehyde was set at 45 s for each stamped enzyme layer and two layers of enzyme were stamped to obtain a rapid response time (~2 s) while still providing good sensitivity and a low detection limit (see below).

### *2.4.5 Biosensor performance*

**Figure 2.5** shows current recordings of a typical biosensor in real time in response to successive step changes in glucose concentration at 0.7 V vs. Ag/AgCl. The biosensor reached 95% of the steady-state current within 2 s in response to changes in glucose concentration, indicating excellent electrocatalytic behavior of the biosensor.

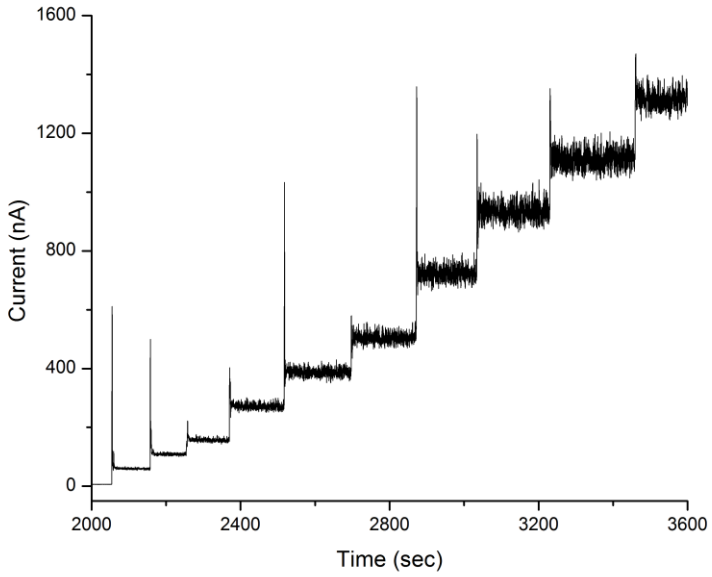


**Figure 2.5** Current response of the biosensor to glucose. The biosensor response in stirred solution was recorded for sequential injections of glucose to give concentrations of 0, 80, 160, 240, 440, 640, 840, 1240, 1640, 2040, 2840, and 3640 μM, at a constant potential of 0.7 V (*vs.* Ag/AgCl) in PBS buffer (pH 7.4).

The apparent Michaelis-Menten constant ($K_m^{app}$), estimated from the non-linear plot of current vs. glucose concentration, was 1.85 ± 0.08 mM (**Figure 2.5** and **Figure 2.6**). The low $K_m^{app}$, which is much lower than the reported range for the free enzyme (*i.e.*, $K_m$ = 33 mM-110 mM) [28-29], likely was due to oxygen-limited enzyme kinetics at glucose concentrations in the millimolar range [30]. Such oxygen limitations at high glucose concentrations, due to relatively low oxygen solubility and mass transfer resistances, causes a reduction in $V_{max}^{app}$, which resulted in the lower $K_m^{app}$ reported here. Further insight into the kinetics was had through a determination of the apparent $k_{cat}$, which is interpreted as the maximum number of substrate molecules converted

to product per enzyme active site per second. The constant, $k_{cat}$, generally is calculated from the quotient of the maximum observed reaction rate and the enzyme concentration, $V_{max}/[E]_0$. In this case, the maximum reaction rate corresponds to the maximum biosensor current observed. For our glucose biosensor, $V_{max}^{app}$ was estimated at ~0.541 nmol $s^{-1}$ $cm^{-2}$ by noting that two electrons are generated for each molecule of $H_2O_2$ oxidized and one molecule of $H_2O_2$ is produced upon enzyme catalyzed oxidation of a molecule of glucose. The GOx concentration and thickness of GOx layer immobilized by PDMS stamping were estimated by FAD extraction followed by fluorescence assays. The surface concentration of the enzyme active sites was estimated at ~2.26 nmol $cm^{-2}$ after two GOx transfers by stamping, which gave the best biosensor performance. Here, the GOx surface concentration estimated from a FAD measurement is based on the assumption that all the FAD-containing, immobilized enzyme is active. With this assumption, $k_{cat}^{app}$ was estimated at ~0.24 $s^{-1}$, which is relatively low [29]. However, this $k_{cat}$ value is an apparent quantity that likely is influenced by mass transport in the electrode coatings and subsequent oxygen limitation at high glucose concentration (see above), and by the fact that most $H_2O_2$ diffuses into the bulk solution (Wang *et al*. 2005). Based on the amount of GOx obtained from FAD experiments and the diameter of the Pt disk electrode, the thickness of the enzyme and BSA layer was estimated to be 7.0 µm. The thickness of one enzyme layer is estimated to be ~3.5 µm, which corresponds to ~435 enzyme molecule layers.

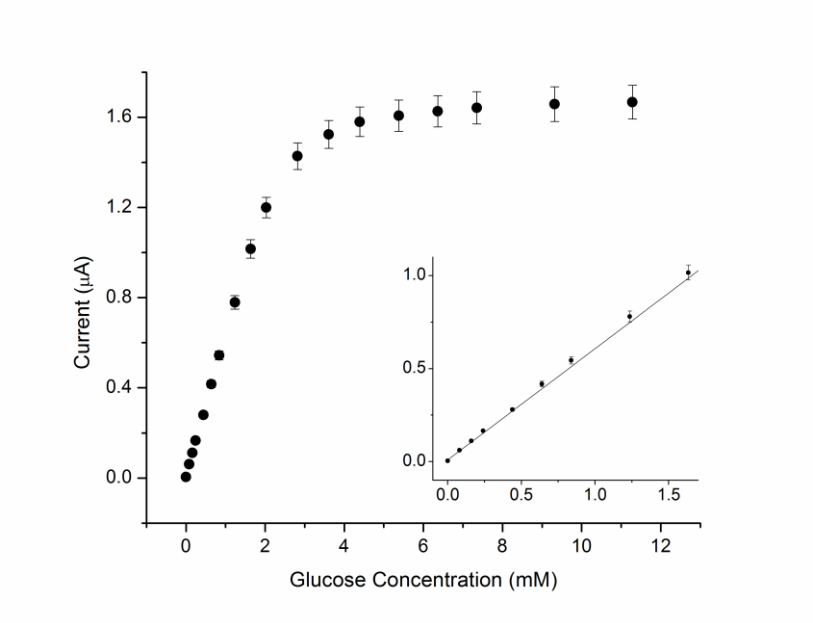


**Figure 2.6** A calibration curve for glucose biosensor. The inset plot shows the lower analyte concentration range. Error bars: standard error of the mean.

A typical calibration curve for the glucose biosensor is presented as **Figure 2.6.** Glucose biosensors fabricated on the same day exhibited a repeatable high sensitivity of 29.4 ± 1.3 μA $mM^{-1}$ $cm^{-2}$ ($n$ = 3) and detection limit of 4.3 ± 1.7 μM ($n$ = 3) at a signal-to-noise ratio of 3. The sensor displayed a linear detection range of up to 2 mM ($R^2$ = 0.998) and a fast response time (~2 s). A larger linear range could be achieved by adding a glucose mass transfer resistance in the form of an additional polymer layer, for example, but this would come at the expense of a longer response time [30]. The performance of our electroenzymatic biosensor fabricated by PDMS stamping compares favorably with recently reported glucose biosensors based on immobilized GOx [31], the best of which tend to rely on more exotic materials including nanoparticles, nanotubes and graphene. For example, Feng *et al.* reported the glucose sensor fabrication by immobilizing GOx into nanostructured graphene-conducting polyaniline nanocomposite [32]. The biosensor showed

some characteristics similar to those reported here (*i.e.*, a sensitivity of 22.1 μA $mM^{-1}$ $cm^{-2}$ and detection limit of 2.769 μM). In further comparison, a sensor utilizing Pt nanoparticles showed a good sensitivity of 17.40 μA $mM^{-1}$ $cm^{-2}$ but a significantly higher limit of detection of 18 μM and slower response time of 15-20 s [33]. The use of maghemite nanoparticles in carbon paste gave rise to a sensor with higher sensitivity, 45.85 μA $mM^{-1}$ $cm^{-2}$, and a lower detection limit of 0.9 μM, but no response time was given [34]. In another report where magnetic nanoparticles were used, a high sensitivity (62.45 μA $mM^{-1}$ $cm^{-2}$) and low detection limit (0.23 μM) also were reported but the response time was ~5 s [35]. Shi and Ma described an amperometric glucose biosensor based on GluOx immobilized in a composite film of silver "nanoprisms" in chitosan. They also reported a relatively high sensitivity of 67.17 μA $mM^{-1}$ $cm^{-2}$ and a more typical detection limit of 1 μM, but the sensor showed "serious" interference from ascorbic acid [3]. Recently, a glucose biosensor constructed of GOx immobilized on chitosan nanoparticles on gold was described that exhibits a response time similar to our biosensor of ≤2 s, yet provides a higher sensitivity of 156.27 μA $mM^{-1}$ $cm^{-2}$ and a lower detection limit of 1.1 μM.[36] However, no selectivity data was given, which is an important consideration for sensors to be used *in vivo* or with biological samples. Another recent review describes the impressive performance characteristics of a number of glucose biosensors based on nanostructured metal oxides including some amperometric electroenzymatic biosensors with several fold higher sensitivity than our biosensor, yet none exhibit a response time of 2 s or less (Rahman *et al*. 2010). Thus, the impressive combination of performance characteristics exhibited by our relatively simple glucose biosensor created with a PDMS stamp appears to be unusual in the recent literature.

## 2.5 Conclusions

In summary, PDMS stamping has proved, for the first time, to be an excellent enzyme deposition method for the preparation of an amperometric glucose biosensor. GOx was successfully transferred onto the electrode surface with its activity retained. The constructed glucose biosensor exhibited high sensitivity (~29 μA $mM^{-1}$ $cm^{-2}$), low detection limit (~4 μM), fast response time (~2 s) and good selectivity. This PDMS stamping method for enzyme transfer may prove especially useful for the high throughput deposition of enzyme at selected sites on microelectrode array microprobes of the kind used for neuroscience research *in vivo*.

## 2.6 References


[1] Zhang, Y. W.; Li, Y. Q.; Wu, W. J.; Jiang, Y. R.; Hu, B. R. Biosens Bioelectron 60 (2014) 271-276.

[2] Tseng, T. T. C.; Monbouquette, H. G. J Electroanal Chem 682 (2012) 141-146.

[3] Shi, W.; Ma, Z. Biosens Bioelectron 26 (2010) 1098-1103.

[4] Nien, P. C.; Tung, T. S.; Ho, K. C. Electroanal 18 (2006) 1408-1415.

[5] Wang, J. J.; Myung, N. V.; Yun, M. H.; Monbouquette, H. G. J Electroanal Chem 575 (2005) 139-146.

[6] Trojanowicz, M.; Krawczyk, T. K. V. Mikrochim Acta 121 (1995) 167-181.

[7] Heller, A.; Feldman, B. Appl. Electrochem. in Med., M. Schlesinger, Ed., Modern Aspects Electrochem. 56 (2013) 121-187.

[8] Hyun, W. J.; Secor, E. B.; Hersam, M. C.; Frisbie, C. D.; Francis, L. F. Adv Mater 27 (2015) 109-115.

[9] Wassum, K. M.; Tolosa, V. M.; Wang, J.; Walker, E.; Monbouquette, H. G.; Maidment, N. T. Sensors 8 (2008) 5023-5036.

[10] Tseng, T. T. C.; Yao, J.; Chan, W.-C. Biochem Eng J 78 (2013) 146-153.

[11] Yi, H. M.; Wu, L. Q.; Bentley, W. E.; Ghodssi, R.; Rubloff, G. W.; Culver, J. N.; Payne, G. F. Biomacromolecules 6 (2005) 2881-2894.

[12] Koev, S. T.; Dykstra, P. H.; Luo, X.; Rubloff, G. W.; Bentley, W. E.; Payne, G. F.; Ghodssi, R. Lab on a Chip 10 (2010) 3026-3042.

[13] Wu, L. Q.; Gadre, A. P.; Yi, H. M.; Kastantin, M. J.; Rubloff, G. W.; Bentley, W. E.; Payne, G. F.; Ghodssi, R. Langmuir 18 (2002) 8620-8625.

[14] Qin, D.; Xia, Y.; Whitesides, G. M. Nature Protocols 5 (2010) 491-502.

[15] Perl, A.; Reinhoudt, D. N.; Huskens, J. Adv Mater 21 (2009) 2257-2268.

[16] Bernard, A.; Renault, J. P.; Michel, B.; Bosshard, H. R.; Delamarche, E. Adv Mater 12 (2000) 1067-1070.

[17] Kane, R. S.; Takayama, S.; Ostuni, E.; Ingber, D. E.; Whitesides, G. M. Biomaterials 20 (1999) 2363-2376.

[18] Yan, L.; Zhao, X. M.; Whitesides, G. M. J Am Chem Soc 120 (1998) 6179-6180.

[19] Xia, Y. N.; Whitesides, G. M. Annu Rev Mater Sci 28 (1998) 153-184.

[20] Bernard, A.; Delamarche, E.; Schmid, H.; Michel, B.; Bosshard, H. R.; Biebuyck, H. Langmuir 14 (1998) 2225-2229.

[21] Wassum, K. M.; Tolosa, V. M.; Tseng, T. C.; Balleine, B. W.; Monbouquette, H. G.; Maidment, N. T. J Neurosci 32 (2012) 2734-2746.

[22] Hamdi, N.; Wang, J. J.; Monbouquette, H. G. J Electroanal Chem 581 (2005) 258-264.

[23] Aggidis, A. G. A.; Newman, J. D.; Aggidis, G. A. Biosens Bioelectron 74 (2015) 243-262.

[24] Walker, E.; Wang, J.; Hamdi, N.; Monbouquette, H. G.; Maidment, N. T. Analyst 132 (2007) 1107-1111.

[25] Lisdat, F.; Schaefer, D. Analytical and Bioanalytical Chemistry 391 (2008) 1555-1567.

[26] Gooding, J. J.; Situmorang, M.; Erokhin, P.; Hibbert, D. B. Anal Commun 36 (1999) 225-228.

[27] Patolsky, F.; Zayats, M.; Katz, E.; Willner, I. Anal Chem 71 (1999) 3171-3180.

[28] Swoboda, B. E. P.; Massey, V. J Biol Chem 240 (1965) 2209-&.

[29] Gibson, Q. H.; Massey, V.; Swoboda, B. E. P. J Biol Chem 239 (1964) 3927-&.

[30] Chen, D. J.; Wang, C.; Chen, W.; Chen, Y. Q.; Zhang, J. X. J. Biosens Bioelectron 74 (2015) 1047-1052.

[31] Martinkova, P.; Pohanka, M. Anal Lett 48 (2015) 2509-2532.

[32] Feng, X.; Cheng, H.; Pan, Y.; Zheng, H. Biosens Bioelectron 70 (2015) 411-417.

[33] Turkmen, E.; Bas, S. Z.; Gulce, H.; Yildiz, S. Electrochim Acta 123 (2014) 93-102.

[34] Baratella, D.; Magro, M.; Sinigaglia, G.; Zboril, R.; Salviulo, G.; Vianello, F. Biosens Bioelectron 45 (2013) 13-18.

[35] Wang, A. J.; Li, Y. F.; Li, Z. H.; Feng, J. J.; Sun, Y. L.; Chen, J. R. Materials Science & Engineering C-Materials for Biological Applications 32 (2012) 1640-1647.

[36] Anusha, J. R.; Raj, C. J.; Cho, B. B.; Fleming, A. T.; Yu, K. H.; Kim, B. C. Sensor Actuat B-chem 215 (2015) 536-543.

# Chapter 3: Implantable Microbiosensor Fabrication by Polydimethylsiloxane Stamping for Combined Amperometric Monitoring of Glucose and Choline

Chapter 3 is a manuscript prepared together with Bonhye Koo.

Bo Wang's contribution to this work focused on microsensor fabrication including acid clean scan, permselective polymer coating, chitosan deposition, biosensor calibration and interferents testing.

## 3.1 Abstract

High performance microprobes for sensing of glucose and choline was fabricated using polydimethylsiloxane (PDMS) microcontact printing (μCP) with alignment for transferring multiple enzymes onto microelectrode arrays of a microprobe. The fabrication process began with polyphenylenediamine (PPD) deposition to block both anionic and cationic interferents (e.g., ascorbic acid and dopamine) found in brain extracellular fluid. A PDMS microstamp as small as the size of the microelectrodes was fabricated based on soft lithography. For a dual sensor fabrication, two model enzymes, choline oxidase (ChOx) and glucose oxidase (GOx), were stamped onto selected microelectrodes in 2 × 2 arrays on a microprobe to demonstrate the successful use of μCP with alignment. The device architecture was examined by optical microscopy and dual-sensing performance was assessed using constant potential amperometry upon sequential injection of choline, glucose, and the interferents. The dual sensor we fabricated showed high sensitivity of choline and glucose (286 and 117 μA/mM $cm^2$, respectively) accompanied by a low detection limit (3 and 1 μA respectively). The work presented here shows the prospects for fabricating a microelectrode array for multiple neurotransmitter sensing and high throughput enzyme deposition.

## 3.2 Introduction

The ability to monitor neurotransmitter release in freely behaving animals is key to understanding neuronal processes underlying complex behaviors. Such behaviors are controlled by neuronal networks employing multiple neurotransmitters. There is an extensive literature pointing to the importance of interactions among more than one neurotransmitter, such as dopamine (DA), glutamate (Glut) and acetylcholine (ACh), in controlling the behaviors. [1-4] Therefore, our understanding of the connection between neurotransmitter releases and behaviors would be greatly facilitated by the capability to monitor *in vivo* multiple neuroactive molecules simultaneously and in near-real time. Existing methods either offer rapid measurements of a single analyte, such as fast-scan cyclic voltammetry, [5-6] or provide multiple analyte measurement with insufficient temporal resolution (microdialysis). [7] There is an extensive literature pointing to the importance of interactions among more than one neurotransmitters such as dopamine (DA), glutamate (Glut) and acetylcholine (ACh), in controlling the behaviors. [1-4] Thus, it will be very important to develop implantable microprobes with an array of microsensors capable of monitoring multiple neurochemicals simultaneously with rapid response time.

We previously reported an implantable probe with arrayed microsensors for combined amperometric monitoring of Glut and DA. However, the glutamate oxidase enzyme used in constructing the glut sensing sites was manually applied to selected microelectrodes, which is very challenging to accomplish given the less than 100 μm spacing between sites and could not be achieved consistently. In contrast, DA is directly electrooxidizable and DA sensing sites were constructed straightforwardly through electrodeposition processes. [8] Clearly, if multiple enzymes are to be deposited on selected microelectrodes on the same microprobe for combined

sensing of for example, glutamate, choline, and glucose, higher resolution, non-manual methods for enzyme transfer and immobilization must be developed.

Microcontact printing (μCP) based on polydimethylsiloxane (PDMS) stamping is an emerging method for transferring proteins to surfaces in high-resolution patterns with feature size down to 500 nm. [9-10] After mold and stamp fabrication, the stamping process first begins by inking a protein solution onto a PDMS stamp. This protein pattern is then transferred onto a target substrate upon contact of the protein-covered PDMS stamp with the surface for a few seconds. The process can be designed to main activity of transferred proteins, and the PDMS stamp can simply be re-used after appropriate cleaning. [9-15].

Previously, we utilized PDMS stamping to transfer glucose oxidase (GOx) onto macroscopic, 1.8-mm-dia. platinum disk electrodes to demonstrate the feasibility of PDMS stamping for fabrication of high performance electroenzymatic biosensors. The glucose biosensors made using PDMS stamping showed excellent properties with a sensitivity of ~29 μA/mM $cm^2$, a detection limit of ~4 μM, and a response time of ~2 s. [16] This work showed the potential of PDMS stamping for transferring concentrated and active enzymes onto electrode surfaces. In this report, we developed PDMS stamping with microscopic alignment to transfer two different enzymes, choline oxidase (ChOx) and GOx, independently onto selected individual sites in a microelecrode array to construct a potentially implantable microprobe for combined sensing of choline and glucose with high sensitivity, low detection limit and rapid response time.

## 3.3 Material and methods

### *3.3.1 Reagents*

Glucose oxidase (from *Aspergillus niger*, CAS NO. 9001-37-0), pyrrole (Py), choline oxidase (Alcaligenes, 9028-67-5), m-phenylenediamine (PD), choline chloride, glutaraldehyde solution (25%), bovine serum albumin (BSA) lyophilized powder, hydrogen peroxide solution (30%), chitosan (from crab shells, minimum 85% deacetylated), D-(+)-glucose, L-ascorbic acid, dopamine hydrochloride, potassium hexacyanoferrate (II) trihydrate, and potassium hexacyanoferrate (III) were purchased from Sigma-Aldrich (St. Louis, MO). Isopropyl alcohol and 1M sulfuric acid solutions were obtained from Fisher Scientific (Pittsburgh, PA). Ag/AgCl glass-bodied reference electrodes with 3 M NaCl electrolyte and 0.5-mm-diameter Pt wire auxiliary electrodes were purchased from BASi (West Lafayette, IN). Sodium phosphate buffer (PBS, pH 7.4) was composed of 50 mM sodium phosphate (dibasic) and 100 mM sodium chloride. Ultrapure water was generated using a Millipore Milli-Q Water System and was used for preparation of all solutions. Four-inch Si wafers were purchased from Silicon Valley Microelectronics (Santa Clara, CA). SU-8 2075 and SU-8 developer were obtained from MicroChem (Westborough, MA). Sylgard® 184 silicone elastomer kit was purchased from Dow Corning (Auburn, MI).

The microelectrodes used in this work were silicon-based multielectrode arrays manufactured at UCLA using microelectro-mechanical-system (MEMS) technologies. The fabrication and array details are described in our previous work.[17-18] The MEA consists of four 6000 $\mu m^2$ (40 $\mu m \times$ 150 $\mu m$) Pt sites, situated in pairs at the tip of a 9-mm-long shank. The pair nearest the shank tip is 100 $\mu m$ from the pair farthest from the shank tip, and the paired sites are 40 $\mu m$ apart. Each site was modified accordingly, to act either as a working, reference, or counter electrode.

### *3.3.2 Instrumentation*

Electrochemical experiments for sensor development, evaluation and calibration were performed using a Versatile Multichannel Potentiostat (model VMP3) equipped with the 'p' low current option and N'Stat box driven by EC-LAB software (Bio-Logic USA, LLC, Knoxville, TN) in a three electrode configuration consisting of the sensing electrode, a Pt wire auxiliary electrode, and a Ag/AgCl glass-bodied reference electrode. A Nova Nano 230 was used for environmental SEM images.

### *3.3.3 Fabrication of mold and polydimethylsiloxane stamps*

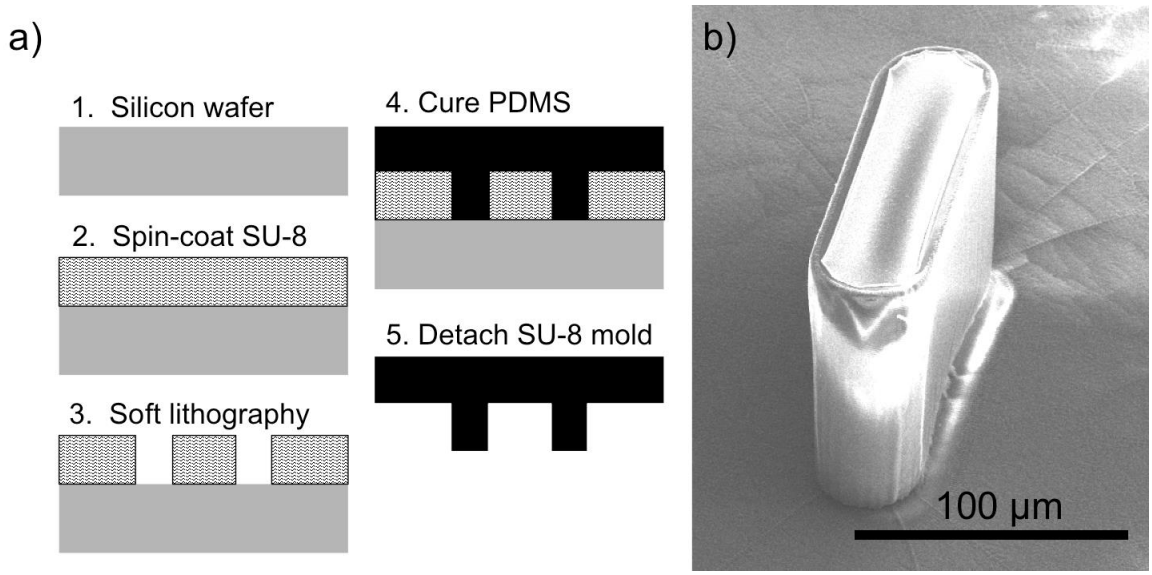


**Figure 3.1** (a) Fabrication process for a SU-8 mold and a PDMS microstamp. (b) Scanning electron microscope (SEM) image of a PDMS microstamp.

The fabrication process for a mold and a PDMS microstamp is illustrated in **Figure 3.1a**. SU-8 2075 was spin-coated on top of a four-inch Si wafer at 2000 rpm for 30 s to give a ~100 µm thick layer. The layer was soft-baked at 65 °C for 5 min and then at 95 °C for 40 min followed by 27 sec of UV exposure (total 216 mJ/cm$^2$). Post exposure baking was done at 65 °C for 5 min and at

95 °C for 10 min. After the layer was patterned in SU-8 developer for 20 min, the mold was cleaned using isopropanol and then left to dry in air at room temperature. Polydimethylsiloxane (PDMS) microstamps were fabricated using the Sylgard® 184 silicone elastomer kit. To cover a 4 inch mold, 6 g of monomer was mixed with 0.6 g of curing agent (1:10; monomer:curing agent) and then centrifuged at 15000 rpm for 5 min to remove air bubbles. After pouring onto the SU-8 mold, the mixture was subsequently degassed under vacuum and cured at 60 °C for 4 h. The PDMS microstamps were detached from the mold and cut into 1 cm × 1 cm pieces. A fabricated PDMS microstamp is shown in **Figure 3.1b**. To ensure that the enzyme mixture is transferred to the entire microelectrode surface (40 μm × 150 μm), the size of a microstamp surface was designed to be 50 μm × 160 μm. The PDMS stamps were cleaned in 7.5 % hydrogen peroxide with sonication and then re-used.

### *3.3.4 Sensor preparation*

Microelectrodes on microprobes were rinsed with isopropyl alcohol followed by an electrochemical cleaning step with 0.5 M sulfuric acid and sonication in ultrapure water. Next, a polyphenylenediamine (PPD) film was electrodeposited (5 mM PD in stirred PBS, 0.85 V vs. Ag/AgCl, 10 min) onto the microelectrode surfaces.

The pH of a chitosan solution (0.04% m/v) was adjusted to pH = 3 using hydrochloric acid (HCl) to dissolve the chitosan flakes. After filtering with a 0.2 μm syringe filter, the pH was adjusted to 5 using sodium hydroxide (NaOH) solution (0.5 M). A constant potential of -0.7 V vs. Ag/AgCl was applied at the PPD-coated Pt electrode surface for 2 min while immersed in the chitosan solution to electrodeposit a chitosan film [19-20].

### *3.3.5 PDMS μCP with alignment*

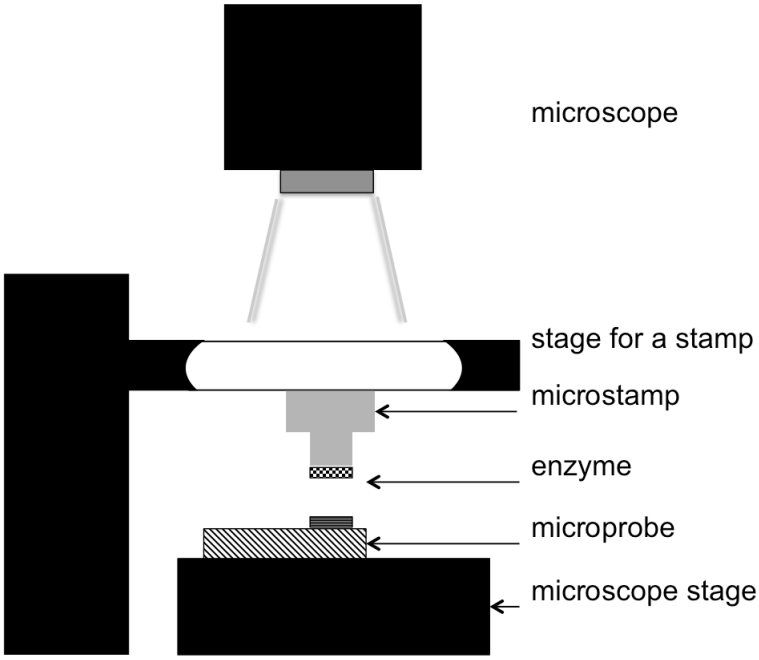


**Figure 3.2** Alignment setup for a PDMS microstamp and a microelectrode on a silicon-based microprobe.

A droplet (3 μL) of enzyme mixture was placed on a PDMS microstamp for ~ 60 min. Enzyme mixtures consisted of ChOx (17.5 mg/mL) or GOx (10 mg/mL) mixed with bovine serum albumin (BSA) in a 1:1 mass ratio in phosphate-buffered saline (PBS). After this inking step, the excess enzyme solution was removed using a Kimwipe, and the microstamp was dried using a nitrogen gun for ~15 s. Since our previous work used a stamp size of 1.6 mm to match with a disk electrode, microscopic alignment was not required for stamping onto the electrode.[16] However, in this work, we aimed to deposit enzyme on selected microelectrodes in a 2 × 2 array on a microprobe where the separation between microelectrodes was 40 μm and 105 μm in the x and y-directions, respectively. As a result, microscopic alignment was necessary for contacting the inked stamp with

selected microelectrodes. The alignment setup consisted of a microscope with an adjustable stage and a separate custom-built, fixed stage to secure the PDMS stamp, as shown in **Figure 2**. The microprobe was attached to the microscope stage and was moved into focus with the surface of the stamp. Alignment of the PDMS microstamp and the target microelectrode was achieved by manipulation of the microscope stage. The microscope stage was then raised further to make contact with the PDMS microstamp. The ChOx mixture and the GOx mixture were stamped onto the upper right and bottom left sites of the microelectrode array. The remaining two microelectrodes, upper left ad bottom right, were left as control sites. The contact time was ~ 1 min to transfer the enzymes from the microstamp to the microelectrode. Subsequently, the microprobe was exposed to vapor from a 5% glutaraldehyde (GAH) solution at room temperature for 1 min to crosslink the chitosan, enzyme and BSA on the microelectrode surfaces. This enzyme stamping and crosslinking process was repeated twice to achieve sufficient enzyme surface concentrations high performance sensing of choline and glucose. The fabricated sensors were preserved at 4 °C under dry conditions when not in use.

### *3.3.6 Electrochemical measurements*

Constant potential amperometric measurements were conducted in PBS buffer at 0.7 V *vs.* Ag/AgCl and at ambient laboratory temperature. More than 30 min of equilibrium time in PBS buffer was allowed to achieve a stable current before adding analytes.

## 3.4 Results and discussion

### *3.4.1 Enzyme layers after PDMS stamping*

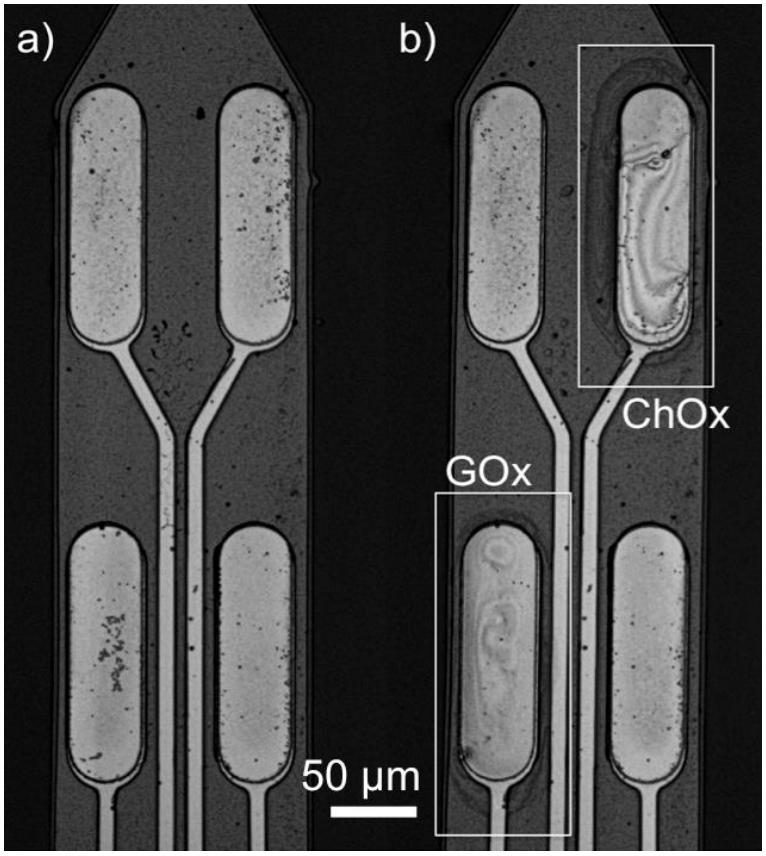


**Figure 3.3** 100× Optical microscope image of microelectrode array of a microprobe (a) before and (b) after PDMS stamping of ChOx and GOx with alignment.

An optical image of the microelectrodes before and after stamping are shown in **Figure 3.3**. A clear deposit of the ChOx and GOx mixtures is evident on the boxed areas of the image (**Figure 3.3b**) that extends slightly beyond the edges of the microelectrode as planned (see Methods). There are no evident surface abnormalities, which implies that alignment and deposition was successful. By increasing the inking time (BSA and enzyme mixture on top of stamp) from previously reported

10 min [16] to 60 min, more consistent enzyme layers were formed resulting in consistent microsensor performance(see below). [8]

### *3.4.2 Glucose microbiosensor performance*

A typical calibration curve for the glucose biosensor is presented as **Figure 3.4.** Glucose biosensors fabricated on the same day exhibited a repeatable high sensitivity of 117 ± 14 μA $mM^{-1}$ $cm^{-2}$ ($n$ = 9) and detection limit of 3 ± 0.5 μM ($n$ = 9) at a signal-to-noise ratio of 3. The sensor displayed a linear detection range of up to 1.44 mM ($R^2$ = 0.9997). The biosensor reached 95% of the steady-state current within 2 s in response to changes in glucose concentration in a stirred beaker, indicating excellent electrocatalytic behavior of the biosensor.

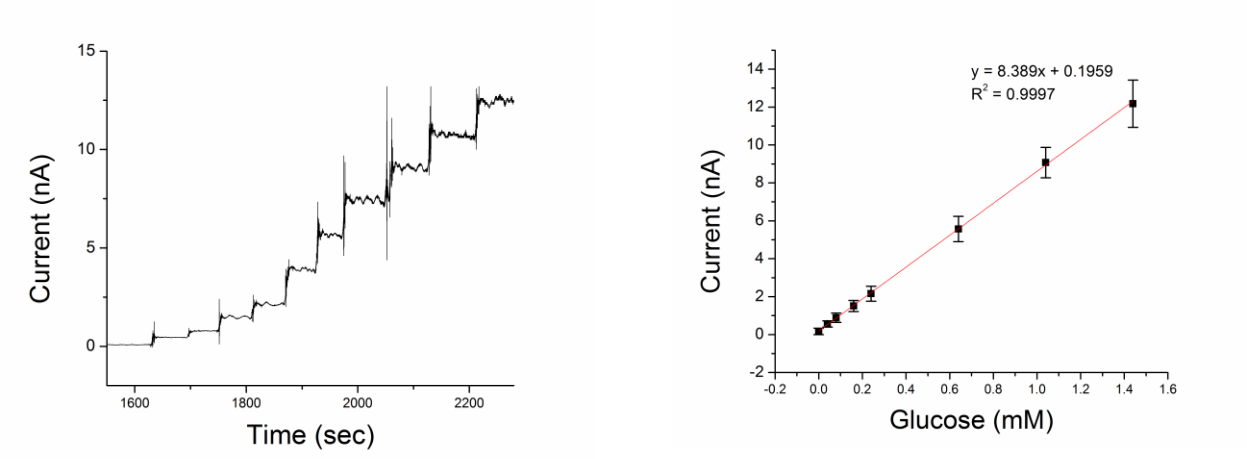


**Figure 3.4** Current response of the biosensor to glucose. The biosensor response in stirred solution was recorded for sequential injections of glucose to give concentrations of 0, 40, 80, 160, 240, 440, 640, 840, 1040, 1240 and 1440 μM, at a constant potential of 0.7 V (*vs.* Ag/AgCl) in PBS buffer (pH 7.4).

In addition, by decreasing glutaraldehyde concentration from 25%, 12.5% to 5% in the solution used for the vapor crosslinking, the best performance was given by 5% glutaraldehyde vapor treatment for 1 min which the sensitivity increased almost 4 times compared to previous reported data (117 vs. 29 μA $mM^{-1}$ $cm^{-2}$). This suggests that excess glutaraldehyde vapor damages the enzyme even during short exposure times of ~1 min.

Compared to recent published articles, the performance of our glucose biosensor lies in the best range (see **Table 3.1**). A recent review describes the impressive performance characteristics of glucose biosensors based on nanostructured metal oxides including some amperometric electroenzymatic biosensors. [21] But besides our fast response time, sensitivity above 100 μA $mM^{-1}$ $cm^{-2}$ was rarely reported for enzymatic glucose biosensors according to the review. Shi and Ma described an amperometric glucose biosensor based on GluOx immobilized in a composite

film of silver "nanoprisms" in chitosan. [22] They also reported a relatively high sensitivity of 67.17 μA $mM^{-1}$ $cm^{-2}$ and a more typical detection limit of 1 μM, but the sensor showed "serious" interference from ascorbic acid (**Table 3.1**). In another article where C-decorated ZnO nanowire was used, a high sensitivity (237.8 μA $mM^{-1}$ $cm^{-2}$) and low detection limit (0.2 μM) also were reported but the response time was ~5 s (**Table 3.1**). [23]

**Table 3.1** Comparison of the performance characteristics of the glucose biosensor of this work with other reported glucose biosensors

| **Enzyme electrodes** | **Sensitivity/ μA $mM^{-1}cm^{-2}$** | **LOD/ μM** | **Response Time /s** | **References** |
|---|---|---|---|---|
| GOx/Chitosan/PPD/Pt | 117 | 3 | ~2 | This work |
| GOx/Chitosan/Nafion/PPy/Pt | 29 | 4 | ~2 | Chapter 2 |
| GOx/Graphene-Polyaniline | 22.1 | 2.77 | ~5 | [24] |
| Chitosan/GOx/Cysteamine/Au | 8.91 | 49.96 | ~9 | [25] |
| GOx/Silver-Chitosan | 67.17 (AA) | 1 | | [22] |
| C-decorated ZnO nanowire | 237.8 | 0.2 | ~5 | [23] |

### *3.4.3 Choline microbiosensor performance*

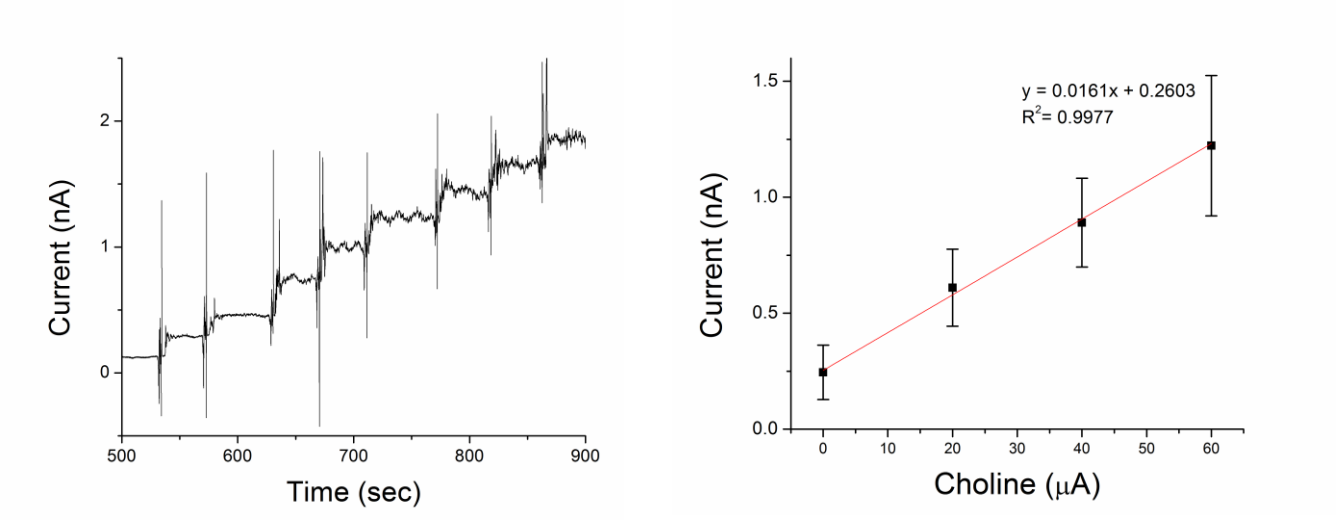


**Figure 3.5** Current response of the biosensor to choline chloride. The biosensor response in stirred solution was recorded for sequential injections of choline chloride to give concentrations of 0, 10, 20, 40, 60, 80, 100, 120, 140 and 160 μM, at a constant potential of 0.7 V (*vs.* Ag/AgCl) in PBS buffer (pH 7.4).

A typical calibration curve for the choline biosensor is presented in **Figure 3.5.** Choline biosensors fabricated on the same day exhibited a repeatable high sensitivity of 286 ± 32 μA $mM^{-1}$ $cm^{-2}$ ($n$ = 4) and detection limit of 1 ± 0.2 μM ($n$ = 4) at a signal-to-noise ratio of 3. The biosensor also displayed a relatively fast response time (~2 s) in a stirred beaker.

**Table 3.2** Comparison of electroanalytical parameters of the proposed biosensor with other reported choline biosensors

| **Enzyme electrodes** | **Sensitivity/ μA $mM^{-1}cm^{-2}$** | **LOD/μM** | **Response Time /s** | **References** |
|---|---|---|---|---|

| | | | | |
|---|---|---|---|---|
| ChOx/Chitosan/PPD/Pt | 286 | 1 | ~2 | This work |
| ChOx/PB/SPE | 110 | 0.5 | 30 | [26] |
| ChOx/IL/MWCNT/GC | 125.8 | 3.85 | | [27] |
| ChOx/Ni-PB/BG/GC | 345.4 | 0.45 | 2 | [28] |
| PDDA/ChOx/ZnO/MWCNT/PG | 178 | 0.3 | | [29] |

Keihan *et al.* reported a very high sensitivity (345.4 μA $mM^{-1}$ $cm^{-2}$) with a low detection limit (0.45 μM), but the biosensors were fabricated by a complex system using multi-walled carbon nanotubes (BCNTs)/ionic liquid (IL)/Prussian blue (PB) nanocomposite modified glassy carbon (GC) electrode. [28] Another article by Ricci *et al.* [26] reported a choline biosensor with a low detection limit (0.5 μM), but with lower sensitivity and longer response time. (**Table 3.2**)

### *3.4.4 Dual sensor and effect of interferents*

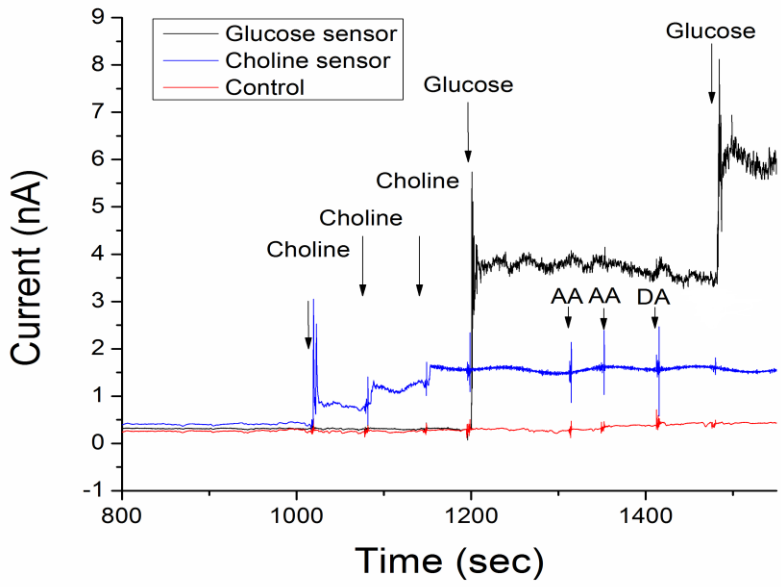

**Figure 3.6** Combined sensing of glucose and choline at a constant potential of 0.7 V (vs. Ag/AgCl). The microprobe was tested in stirred PBS solution upon sequential injections to give 20 μM, 40 μM and 60 μM of choline chloride, 0.6 mM of glucose, 250 μM and 500 μM of ascorbic acid (AA), 5 μM of dopamine (DA) and 1.2 mM of glucose.

**Figure 3.6** shows the combined sensing of glucose and choline by our microprobe with separate biosensing sites for the two analytes that were created using PDMS stamping. The glucose and choline microbiosensor selectivity was tested with ascorbic acid and dopamine, common electrooxidizable interferents found in brain extracellular fluid. (**Figure 3.6**) Physiologically relevant concentrations of 5 μM dopamine and 250 and 500 μM ascorbic acid were used, and a negligible biosensor response was observed at the constant operating potential of 0.7 V (vs. Ag/AgCl) (**Figure 3.6**), although the appropriate biosensing sites exhibited the expected responses to hydrogen peroxide and to glucose or choline. These results show that polyphenylenediamine blocks access of these key electroactive interferents, which suggests that this microprobe may be a useful implantable tool for neuroscience research.

## 3.5 Conclusions

PDMS stamping has been employed successfully for microbiosensor fabrication at selected sites in a microarray on an implantable microprobe. The microbiosensor sites showed high sensitivity for choline and glucose (286 and 117 μA/mM $cm^2$, respectively), a fast response time (~2 s in both cases), and a low detection limit (3 and 1 μA, respectively). The PDMS microstamping technique is expected to contribute to neuroscience research by enabling the

controlled deposition of different enzymes on selected microelectrode sites on a microprobe thereby enabling the combined sensing of multiple neurochemicals at the same location simultaneously. The high resolution and non-manual nature of this stamping approach for enzyme transfer also should enable a decrease in size of the microelectrode arrays in order to minimize tissue damage and increase spatial resolution, as well as a higher throughput process to generate microprobes for combined electroenzymatic sensing of multiple analytes.

## 3.6 References


[1] Lapish, C. C.; Seamans, J. K.; Chandler, L. J. Alcohol Clin Exp Res 30 (2006) 1451-1465.

[2] Andre, V. M.; Cepeda, C.; Levine, M. S. Cns Neuroscience & Therapeutics 16 (2010) 163-178.

[3] Andre, V. M.; Cepeda, C.; Cummings, D. M.; Jocoy, E. L.; Fisher, Y. E.; Yang, X. W.; Levine, M. S. Eur J Neurosci 31 (2010) 14-28.

[4] Cepeda, C.; Andre, V. M.; Yamazaki, I.; Wu, N. P.; Kleiman-Weiner, M.; Levine, M. S. Eur J Neurosci 27 (2008) 671-682.

[5] Robinson, D. L.; Venton, B. J.; Heien, M.; Wightman, R. M. Clin Chem 49 (2003) 1763-1773.

[6] Pihel, K.; Walker, Q. D.; Wightman, R. M. Anal Chem 68 (1996) 2084-2089.

[7] V.I. Chefer, A. C. T., A. Zapata, T.S. Shippenberg Curr. Protoc. Neurosci. 2 (2009) 7.1.1-7.1.28.

[8] Tseng, T. T.; Monbouquette, H. G. J Electroanal Chem (Lausanne Switz) 682 (2012) 141-146.

[9] Bernard, A.; Delamarche, E.; Schmid, H.; Michel, B.; Bosshard, H. R.; Biebuyck, H. Langmuir 14 (1998) 2225-2229.

[10] Perl, A.; Reinhoudt, D. N.; Huskens, J. Adv Mater 21 (2009) 2257-2268.

[11] Qin, D.; Xia, Y.; Whitesides, G. M. Nature Protocols 5 (2010) 491-502.

[12] Bernard, A.; Renault, J. P.; Michel, B.; Bosshard, H. R.; Delamarche, E. Adv Mater 12 (2000) 1067-1070.

[13] Kane, R. S.; Takayama, S.; Ostuni, E.; Ingber, D. E.; Whitesides, G. M. Biomaterials 20 (1999) 2363-2376.

[14] Yan, L.; Zhao, X. M.; Whitesides, G. M. J Am Chem Soc 120 (1998) 6179-6180.

[15] Xia, Y. N.; Whitesides, G. M. Annu Rev Mater Sci 28 (1998) 153-184.

[16] Bo Wang, B. K., Harold G. Monbouquette (2016).

[17] Wassum, K. M.; Tolosa, V. M.; Wang, J.; Walker, E.; Monbouquette, H. G.; Maidment, N. T. Sensors 8 (2008) 5023-5036.

[18] Wassum, K. M.; Tolosa, V. M.; Wang, J. J.; Walker, E.; Monbouquette, H. G.; Maidment, N. T. Sensors 8 (2008) 5023-5036.

[19] Tseng, T. T. C.; Yao, J.; Chan, W.-C. Biochem Eng J 78 (2013) 146-153.

[20] Wu, L. Q.; Gadre, A. P.; Yi, H. M.; Kastantin, M. J.; Rubloff, G. W.; Bentley, W. E.; Payne, G. F.; Ghodssi, R. Langmuir 18 (2002) 8620-8625.

[21] Rahman, M. M.; Ahammad, A. J. S.; Jin, J. H.; Ahn, S. J.; Lee, J. J. Sensors 10 (2010) 4855-4886.

[22] Shi, W. T.; Ma, Z. F. Biosens Bioelectron 26 (2010) 1098-1103.

[23] Liu, J. P.; Guo, C. X.; Li, C. M.; Li, Y. Y.; Chi, Q. B.; Huang, X. T.; Liao, L.; Yu, T. Electrochem Commun 11 (2009) 202-205.

[24] Feng, X.; Cheng, H. J.; Pan, Y. W.; Zheng, H. Biosens Bioelectron 70 (2015) 411-417.

[25] Zhang, Y. W.; Li, Y. Q.; Wu, W. J.; Jiang, Y. R.; Hu, B. R. Biosens Bioelectron 60 (2014) 271-276.

[26] Ricci, F.; Amine, A.; Palleschi, G.; Moscone, D. Biosens Bioelectron 18 (2003) 165-174.

[27] Rahimi, P.; Ghourchian, H.; Sajjadi, S. Analyst 137 (2012) 471-475.

[28] Keihan, A. H.; Sajjadi, S.; Sheibani, N.; Moosavi-Movahedi, A. A. Sensor Actuat B-chem 204 (2014) 694-703.

[29] Zhang, H.; Yin, Y. J.; Wu, P.; Cai, C. X. Biosens Bioelectron 31 (2012) 244-250.

# Chapter 4: An Implantable Electroenzymatic Choline Microsensor by Introducing Nanostructured Platinum

Chapter 4 is a manuscript prepared together with Lili Feng.

Bo Wang's contribution to this work focused on biosensor calibration, interferents testing and Pt nanograss coating.

## 4.1 Abstract

A microelectrode array microprobe with a choline sensing site and an on-probe reference electrode was constructed by depositing permselective polymer films and choline oxidase, and IrOx, respectively, on Pt microelectrodes coated with a nanostructured Pt deposit. The nanostructured Pt coating was deposited from a solution of $H_2PtCl_6$ and formic acid at reducing potential and the organized structure of the deposit, as observed by scanning electron microscopy, is referred to as Pt nanograss. Polyphenylenediamine (PPD) and Nafion were coated sequentially on the working (i.e., sensing) electrode surface to serve as permselective polymers. The choline sensor was tested at physiological concentrations of electroactive interfering species common to brain extracellular fluid (i.e., ascorbic acid, dopamine, DOPA, and DOPAC) and choline. The microsensor with on-probe IrOx reference showed high sensitivity (~123 μA $mM^{-1}$ $cm^{-2}$), low detection limit (~3 μM), fast response time (~3-5 s) and excellent selectivity. Selectivity likely was aided by the relatively low potential of 0.35 V *vs.* IrOx that was made possible by the apparently enhanced $H_2O_2$ electrooxidation activity of the underlying Pt nanograss-coated working electrode. Therefore, Pt nanograss appears to be an excellent Pt surface modification for creation of electroenzymatic biosensors for *in vivo* applications.

## 4.2 Introduction

Choline is a precursor and metabolite of the neurotransmitter acetylcholine. It can serve as a surrogate for acetylcholine measurement due to the rapid hydrolysis of acetylcholine to choline catalyzed by acetylcholine esterase in the brain. Therefore, the monitoring of choline is of importance to neuroscience, especially in the study of Alzheimer'sand Parkinson's diseases. Among the various methods available for choline sensing, amperometric choline oxidase (ChOx)-based biosensors have attracted considerable attention due to their simplicity, rapid response, high sensitivity and low cost. In these biosensors [1-4], choline detection is achieved by electrooxidation of the $H_2O_2$ produced during oxidation of choline catalyzed by choline oxidase:

$$\text{Choline} + 2O_2 + H_2O \xrightarrow{\text{ChOx}} \text{betaine} + 2H_2O_2$$

However, a drawback of this method is the high potential normally used for $H_2O_2$ electrooxidation. Many electroactive interfering substances present in brain extracellular fluid such as ascorbic acid (AA) dopamine (DA) can be electrooxidized at the potentials used to give false current signals. In order to solve this problem, several approaches have been explored to biosensor design for reduction of interference. Modification of the electrode surface by polymetric memberane permeable to $H_2O_2$ and impermeable to interfering species is one of the most effective methods to address this problem. For example, overoxidized polypyrrole (OPPy) could be used to reject DA. [5-6] The perfluoronated ionomer, Nafion, is commonly used to exclude anionic interferents.[7]

Alternative method that are not dependent on permseletive species had also been explored, such as operating at reducing potentials sufficient for $H_2O_2$ reduction using an extra enzyme

horseradish peroxidase or redox mediators.[8] However, the response of the mediated biosensors also faces challenges such as oxidation promotion of interferents by some mediators themselves.

By using some surface modification materials (such as Pt black) to enlarge the surface area may also result in potential reduction. Pt black has been shown to be one of the best electrode materials for oxidation of $H_2O_2$. [9] Hamdi *et al.* [10] demonstrated that by depositing Pt black on a Pt wire to be used for glutamate microsensor fabrication, the sensor working potential could be set at 0.45 V versus Ag/AgCl (as opposed to ~0.7 V in the usual case with polished Pt electrodes) without a loss in sensor performance. It was also mentioned that the good performance at reduced working potential is due at least partially to altered catalytic properties and is not merely the result of an increase in the electroative surface area. [11] However, practical applicability of Pt black is limited as a consequence of its low mechanical stability. [12-14] In addition, Pt black has been reported to cause a cytotoxic reaction presumably due to elution of traces of lead that were used in the fabrication of the deposit.[15]

Recently, Boehler *et al.* introduced a nanostructured Pt-coating. [16] In comparison to Pt black deposition, all chemicals used in this deposition process are non-cytotoxic. The grass-like nanostructure was found to reduce the impedance by almost two orders of magnitude compared to bare polished electrode surfaces. The Pt-grass coating method is performed via a simple electrochemical process that can be applied to virtually any possible electrode type and accordingly shows potential as a universal impedance reduction strategy. Their elution tests revealed non-toxicity of the Pt-grass and the coating was found to exhibit strong adhesion to the metallized substrate. Thus, the nanostructured Pt-coating could be an excellent replacement for Pt black provided it also enables operation of $H_2O_2$ sensing electrodes at reduced potential.

Smaller electrodes used for neurochemical monitoring *in vivo* cause reduced tissue damage and provide improved spatial and temporal resolution. However, in conjunction with the sensing electrode (the working electrode) a reference electrode (RE) must be provided to complete an electrochemical sensing system. Currently, a separate RE, typically Ag/AgCl is used in most *in vivo* studies.[17-21] However, Ag/AgCl is unstable, causes an inflammatory response and requires a separate penetration into the brain. Recently, Tolosa *et al.* reported the construction of a biocompatible iridium oxide (IrOx) RE on the same microprobe with the multielectrode sensing array.[22] [23-25] The reported multielectrode sensing device with on-probe reference showed reduced baseline noise, by an average of ~61% *in vitro* and ~71% *in vivo* with reduced tissue damage, which can result in improved detection limits.

Currently, we are fabricating an implantable, micromachined microprobe with a microsensor array for monitoring of multiple neurotransmitters, including glutamate (Glut), choline, and dopamine (DA), by constant potential amperometry. [26] This study focuses on the creation of an improved choline microsensor based on an underlying Pt electrode with a nanostructured Pt-coating. This Pt-coating also was used in the construction of a high surface area on-probe reference electrode. We demonstrate that this nanostructure Pt coating provides a feasible approach for construction of electoenzymatic microsensors operable at reduced potential and of biocompatible, on-probe REs that reduce noise and tissue damage.

## 4.3 Material and methods

### *4.3.1 Materials*

Choline oxidase (Alcaligenes, 9028-67-5), m-phenylenediamine, Nafion® (5%), glutaraldehyde solution (25%), bovine serum albumin (BSA) lyophilized powder, 3,4-dihydroxyphenylacetic acid, 3,4-dihydroxy-DL-phenylalanine, (-)-epinephrine (+)-bitartrate salt, DL-norepinephrine hydrochloride, serotonin hydrochloride, hydrogen peroxide solution (30%), choline hydrochloride, D-(+)-glucose, iridium tetrachloride hydrate, oxalic acid dehydrate (99%); L-ascorbic acid, dopamine hydrochloride, formic acid, chloroplatinic acid hexahydrate were purchased from Sigma-Aldrich (St. Louis, MO). Isopropyl alcohol and 1M sulfuric acid solution were obtained from Fisher Scientific (Pittsburgh, PA). Ag/AgCl glass-bodied reference electrodes with 3 M NaCl electrolyte, 0.5-mm-diameter Pt wire auxiliary electrodes and disk Pt electrodes (1.6 mm dia.) were purchased from BASi (West Lafayette, IN). Sodium phosphate buffer (PBS, pH 7.4) was composed of 50 mM sodium phosphate (dibasic) and 100 mM sodium chloride. Ultrapure water was generated using a Millipore Milli-Q Water System and was used for preparation of all solutions.

### *4.3.2 Instrumentation and electrochemical measurements*

Electrochemical measurements were performed using a Versatile Multichannel Potentiostat equipped with the ‘p’ low current option and low current N0 stat box (VMP3, Bio-Logic USA LLC, Knoxville, TN, USA) or a multichannel FAST-16 potentiostat (Quanteon, LLC, Lexington, KY, USA). A standard three-electrode system was used with the VMP3 system, consisting of either an on-probe Pt site or a separate Pt-wire as a counter electrode; modified sites on our MEA as the working electrodes; and as RE, either an on-probe IrOx site or a separate AgCl-coated Ag

wire (Bioanalytical Systems, Inc., West Lafayette, IN, USA. Constant potential amperometric measurements were conducted in PBS buffer either at 0.45 V vs. Ag/AgCl or 0.35 V vs. on-probe IrOx reference electrode at ambient laboratory temperature. Sufficient equilibration time in PBS buffer was required to achieve a stable current before adding analytes. A Nova 600 was used for SEM images. A Nova 600 was used for SEM images.

### *4.3.3 Microsensor preparation*

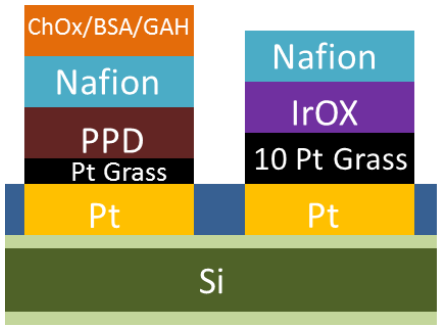


**Figure 4.1** Schematic diagram of the choline sensor configuration.The left site is the choline working electrode coated with Pt nanograss, PPD, Nafion and enzyme layers. The right site is the IrOx reference electrode coated with Pt grass (10 times concentrated Pt nanograss solution was used), IrOx and Nafion.

The microelectrodes used in this work were silicon-based multielectrode arrays manufactured at UCLA using microelectro-mechanical-system (MEMS) technologies. The fabrication and array details are described in previous work.[27-28] The MEA consists of four ~6000 $\mu m^2$ Pt sites, situated in pairs at the tip of a 9-mm-long shank. The pair nearest the shank tip is 100 μm from the

pair farthest from the shank tip, and the paired sites are 40 μm apart. Each site was modified accordingly, to act either as a working, reference, or counter electrode.

The platinum nanograss was deposited in a chemical reduction reaction using an aqueous solution of 2.5 mM $H_2PtCl_6$ and 1.5 mM formic acid (1× solution) and 25 mM $H_2PtCl_6$ and 15 mM formic acid (10× solution). Pt-grass formation was conducted potentiostatically from the $H_2PtCl_6$ solution at -0.1 V vs Ag/AgCl for 300 s.[16] For the reference electrode, IrOx was electrodeposited following the method described by Yamanaka *et al.* and Tolosa *et al.* [22,29] after Pt nanograss deposition. [22] For Pt black deposition, a deposit was forced on the cleaned electrodes by cycling potential between 1.4 and 2.0 V at 500 mV/s for a total of 15 cycles in a vigorously stirred plating solution. The plating solution consisted of 1% chloroplatinic acid, 0.0025% HCl, and 0.01% lead acetate in water, which was Ar-purged for 15 min prior to use. [10]

The choline sensing microelectrodes were created according to the general guidelines of our previously developed procedure except that PPD was electrodeposited instead of polypyrrole (PPy) from a solution of 5 mM PD in PBS (pH 7.4) by holding the voltage constant at 0.85 V for 5 min. The anionic polymer, Nafion, was deposited on all sites by rapid dip-coating of the probe tips in the Nafion solution and oven-casting at 175 °C for 4 min, followed by a 3-min cooling period in ambient air. After the polymer treatments, enzyme immobilization by chemical crosslinking was accomplished using a solution consisting of ChOx (0.33 unit/μL), BSA (20 μg/μL) and glutaraldehyde ($5 \times 10^{-3}$ μL/μL). While working under a microscope, a small drop of the solution was formed on a syringe tip and the drop was gently swiped across the bottom two microelectrode sites at the probe tip. Apply another swipe after the surface was dry. This swipe was repeated eleven more times. The resultant working electrodes (WEs) were used to sense choline by electroenzymatic amperometry.

Microelectrode sites coated with Pt grass, PPD, Nafion and ChOx are referred to here as the working electrode (WE). In contrast, microelectrode sites coated with Pt grass, IrOx and Nafion are referred to here as on-probe reference electrode (RE). The biosensors were sealed in a container with desiccant and stored dry at 4 °C for 48 h prior to testing. **Figure 4.1.** is a schematic diagram showing the configuration of the working electrode and reference electrode.

## 4.4 Results and discussion

### *4.4.1 Surface morphologies of Pt nanograss and Pt black*

The surface morphologies of Pt nanograss and Pt black were imaged by SEM. As shown in **Figure 4.2** (a)-(d), Pt nanograss was grown from the surface and has a well-organized structure similar to that shown by Boehler *et al.* [16] Compared to 1× Pt nanograss (deposition from 1× solution, **Figure 4.2** (a) and (b)), 10× Pt nanograss (deposition from 10× solution, **Figure 2** (c) and (d)) appears thicker with a more uniform pillar-like structure. On the other hand, Pt black appears as an irregular, nonuniform deposit, **Figure 4.2** (e) and (f). This difference in the structure could explain the superior mechanical stability of Pt nanograss compared to Pt black, whose practical applicability is limited as a consequence. Also, the random structure of Pt black could be a source of the excessive noise observed with electrodes coated with this material. In addition, Pt black-coated electrodes were reported to be cytotoxic due to traces of lead remaining from the deposition process.[15] In contrast the biocompatibility of the Pt-nanograss coating was validated by Boehler *et al.*[16]

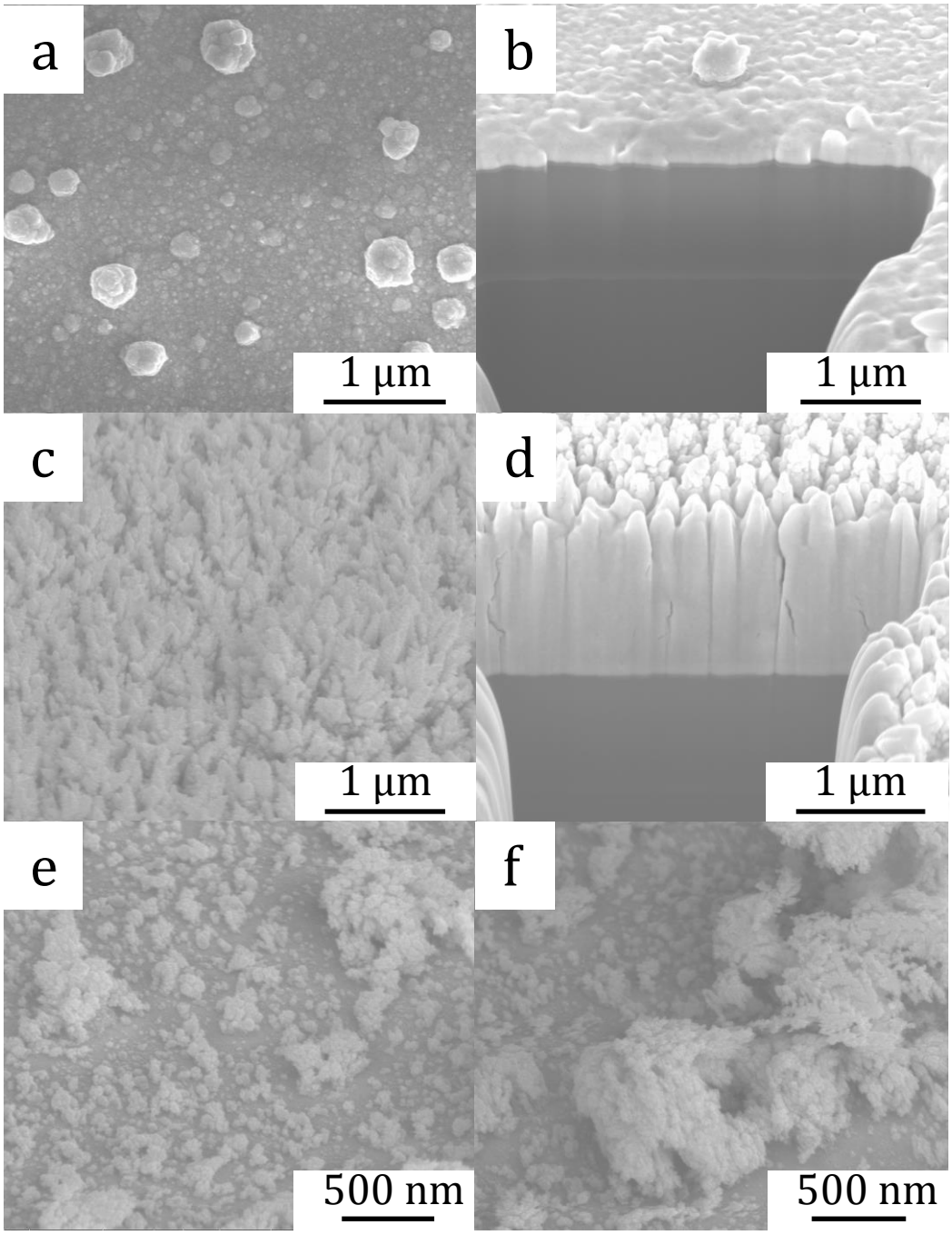


**Figure 4.2** Scanning electron microscopic (SEM) images of (a) Top view of Pt/Pt-nanograss (from 1× solution), (b) Cross section view of Pt/Pt-nanograss (from 1× solution) (c) Angled top view of Pt/Pt-nanograss (from 10× solution), (d) Cross section view of Pt/Pt-nanograss (from 10× solution), and (e, f) Angled top view of Pt black.

### *4.4.2 Pt naograss utilized for working electrode and Ag/AgCl as reference electrode*

A working electrode was coated with 1× Pt nanograss, followed by PPD, Nafion and an enzyme coating. The enzyme mixture was prepared without choline oxidase for a control site. After testing choline microbiosensor with choline at different voltages, it was observed that at potentials of 0.45 V and higher, the sensitivity remains essentially constant. At potentials lower than 0.45 V, the sensitivity decreased modestly. Thus, the working potential for further study was set at 0. 45 V.

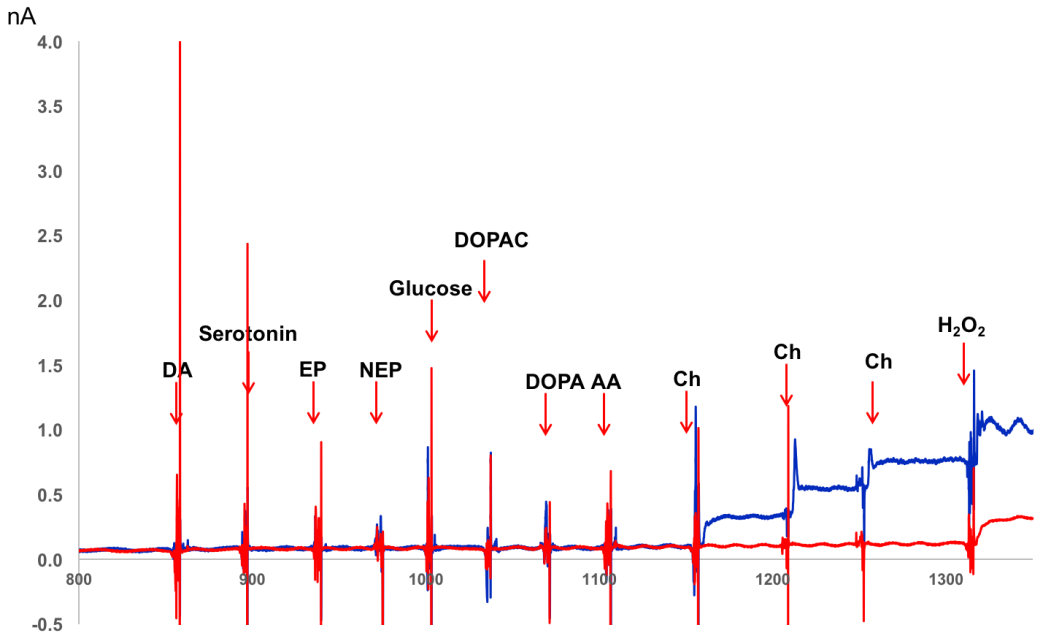


**Figure 4.3** Current response of the choline biosensor to electroactive interferents, choline, and $H_2O_2$. The biosensor response at a constant potential of 0.45 V (*vs.* Ag/AgCl) was monitored in stirred solution upon sequential injections to give 12.5 µM DA, 5 µM Serotonin, 12.5 µM EP, 12.5 µM NEP, 0.8 mM Glucose, 50 µM DOPAC, 50 µM DOPA, 250 µM AA, followed by 20 µM, 40

μM and 60 μM of choline (Ch), and 20 μM of hydrogen peroxide ($H_2O_2$). Control site: red, Pt grass/PPD/Nafion/BSA; Choline sensor site: blue: Pt grass/PPD/Nafion/ChOx-BSA.

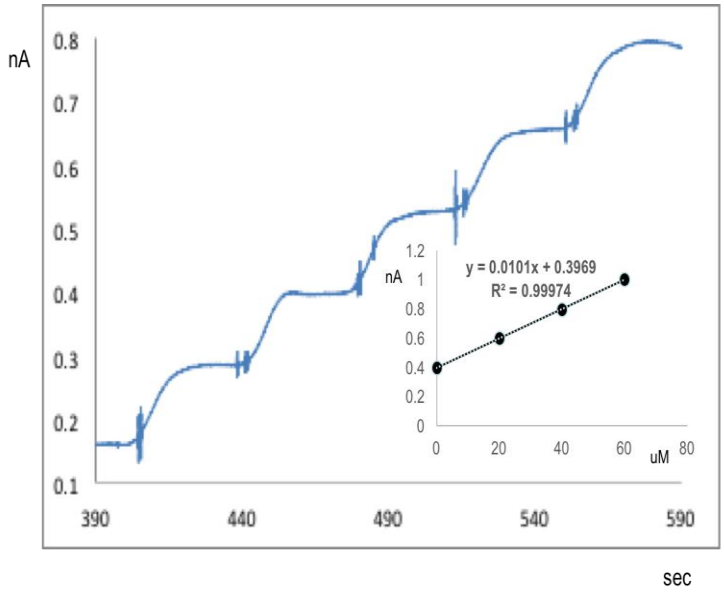


**Figure 4.4** A calibration curve for choline sensor (Ag/AgCl as external RE).The biosensor response at a constant potential of 0.45 V (*vs.* Ag/AgCl) was monitored in stirred solution upon sequential injections to give 10 μM, 20 μM, 30 μM, 40 μM, 50 μM and 60 μM choline.

A typical calibration curves for the choline microsensor with underlying Pt nanograss coating is presented in **Figure 4.4.** The choline sensor has a sensitivity of 196 ± 16 μA $mM^{-1}$ $cm^{-2}$ (n = 4) and a detection limit of 2 ± 0.3 μM (n = 4) at a signal-to-noise ratio of 3 for choline and a response time of 3-5 s. The sensor displayed a linear range up to 196 μM.

### *4.4.3 IrOx as reference electrode*

In order to fabricate an all-in-one choline microbiosensor, which could be used conveniently without an external reference electrode (*e.g.* Ag/AgCl), IrOx was introduced as an on-probe

reference electrode. Tolosa *et al.* recently reported an implantable micromachined multi-electrode array (MEA) microprobe modified for utilization as a complete electrochemical biosensor for rapid glutamate detection.[22] After 10× Pt nanograss deposition onto a Pt microelectrode surface, IrOx was deposited for making reference electrode. Pt nanograss coated at 1× concentration was found to REs with unsatisfactory performance including an unstable current response at the choline sensor site at higher analyte concentration.

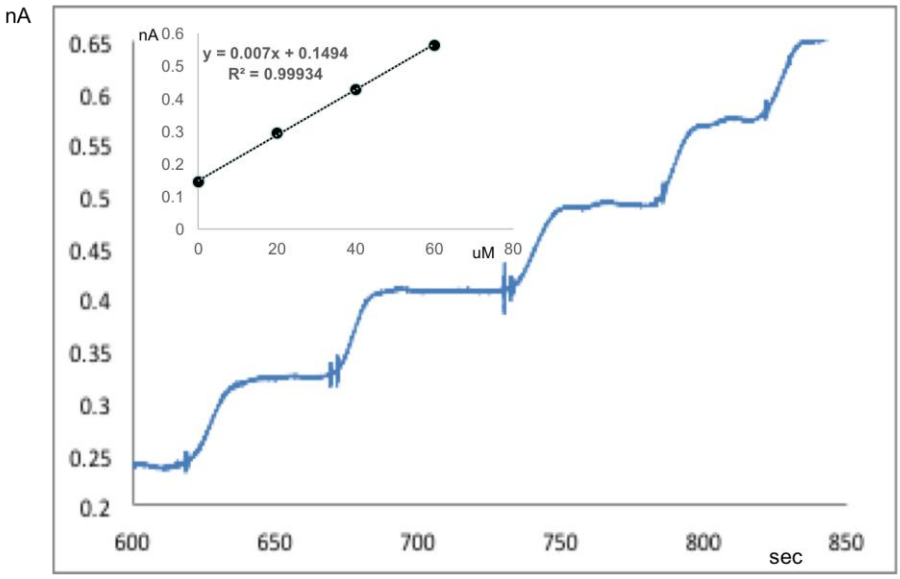


**Figure 4.5** A calibration curve for choline sensor with an IrOx as on-probe RE. The biosensor response at a constant potential of 0.35 V (*vs.* IrOx) was monitored in stirred solution upon sequential injections to give 10 μM, 20 μM, 30 μM, 40 μM, 50 μM and 60 μM.

A calibration curve for the choline sensor with Pt nanograss-coated Pt used in constructing the working and reference electrodes are presented in **Figure 4.5** It should be noted that 0.35 V (vs. IrOx) corresponds to ~0.45 V (vs. Ag/AgCl). The choline sensor exhibited a 123 ± 11 μA $mM^{-}$

$^{1}$ $cm^{-2}$ (n = 4) and a detection limit of 3 ± 0.7 μM (n = 4) at a signal-to-noise ratio of 3. The sensor displayed a detection range up to 138 μM for choline and a response time of 3-5s.

### *4.4.4 Effect of interferents*

The selectivity of the choline biosensors was evaluated. All fabricated biosensors (using external Ag/AgCl RE or on-probe IrOx RE) showed no response to common interferents of brain extracellular fluid at (or more than) physiological concentrations. The sensors were tested with 12.5 μM DA, 5 μM Serotonin, 12.5 μM EP, 12.5 μM NEP, 0.8 mM Glucose, 50 μM DOPAC, 50 μM DOPA, 250 μM AA at constant potential of 0.45 V *vs.* Ag/AgCl or 0.35 V *vs.* IrOx) and no obvious response was observed with the injections (see **Figure 4.3**). This indicates that PPD and Nafion effectively block the access of electroactive interferents commonly encountered in brain extracellular fluid at the relatively low operating potentials used.

## 4.5 Conclusions

In summary, a high performance all-in-one electroenzymatic choline microsensor was fabricated by introducing nanostructured platinum as an underlying Pt coating. The working potential was adjusted to 0.45 V (vs. Ag/AgCl) instead of commonly used 0.7 V (vs. Ag/AgCl). The developed biosensor (either using external or on-probe reference IrOx electrode) demonstrated great performance in high sensitivity, low detection limit, fast response time and good selectivity. Pt nanograss coating was proved to be a perfect replacement for Pt black which is cytotoxic. The choline biosensor could be used for *in vivo* studies.

## 4.6 References


[1] Keihan, A. H.; Sajjadi, S.; Sheibani, N.; Moosavi-Movahedi, A. A. Sensor Actuat B-chem 204 (2014) 694-703.

[2] Baker, K. L.; Bolger, F. B.; Lowry, J. P. Analyst 140 (2015) 3738-3745.

[3] Mazurenko, I.; Tananaiko, O.; Biloivan, O.; Zhybak, M.; Pelyak, I.; Zaitsev, V.; Etienne, M.; Walcarius, A. Electroanal 27 (2015) 1685-1692.

[4] Santos, R. M.; Laranjinha, J.; Barbosa, R. M.; Sirota, A. Biosens Bioelectron 69 (2015) 83-94.

[5] Tseng, T. T. C.; Monbouquette, H. G. J Electroanal Chem 682 (2012) 141-146.

[6] Lowry, J. P.; Oneill, R. D. Electroanal 6 (1994) 369-379.

[7] Gerhardt, G. A.; Oke, A. F.; Nagy, G.; Moghaddam, B.; Adams, R. N. Brain Res 290 (1984) 390-395.

[8] Kulagina, N. V.; Shankar, L.; Michael, A. C. Anal Chem 71 (1999) 5093-5100.

[9] Khan, G. F.; Wernet, W. J Electrochem Soc 143 (1996) 3336-3342.

[10] Hamdi, N.; Wang, J. J.; Walker, E.; Maidment, N. T.; Monbouquette, H. G. J Electroanal Chem 591 (2006) 33-40.

[11] Ryan, M. R.; Lowry, J. P.; Oneill, R. D. Analyst 122 (1997) 1419-1424.

[12] Sharanya Arcot Desai, J. D. R., Liang Guo, and Steve M. Potter Front Neuroengineering 3 (2010) 1-5.

[13] Tang, R. Y.; Pei, W. H.; Chen, S. Y.; Zhao, H.; Chen, Y. F.; Han, Y.; Wang, C. L.; Chen, H. D. Science China-Information Sciences 57 (2014).

[14] ROBINSON, D. A. P IEEE 56 (1968) 1065-1071.

[15] Schuettler M, D. T., Wien SL, Becker S, Staiger A, Hanauer M, Kammer S, Stieglitz T 10th Annual Conference of the International FES Society, Montreal, Canada (2005).

[16] Boehler, C.; Stieglitz, T.; Asplund, M. Biomaterials 67 (2015) 346-353.

[17] Hu, Y. B.; Mitchell, K. M.; Albahadily, F. N.; Michaelis, E. K.; Wilson, G. S. Brain Res 659 (1994) 117-125.

[18] Lee, K. H.; Kristic, K.; van Hoff, R.; Hitti, F. L.; Blaha, C.; Harris, B.; Roberts, D. W.; Leiter, J. C. Brain Res 1162 (2007) 121-129.

[19] Thomas, T. C.; Grandy, D. K.; Gerhardt, G. A.; Glaser, P. E. A. Neuropsychopharmacol 34 (2009) 436-445.

[20] Walker, E.; Wang, J.; Hamdi, N.; Monbouquette, H. G.; Maidment, N. T. Analyst 132 (2007) 1107-1111.

[21] Wassum, K. M.; Tolosa, V. M.; Tseng, T. C.; Balleine, B. W.; Monbouquette, H. G.; Maidment, N. T. J Neurosci 32 (2012) 2734-2746.

[22] Tolosa, V. M.; Wassum, K. M.; Maidment, N. T.; Monbouquette, H. G. Biosens Bioelectron 42 (2013) 256-260.

[23] Yuen, T. G. H.; Agnew, W. F.; Bullara, L. A. Biomaterials 8 (1987) 138-141.

[24] Tivol, W. F.; Agnew, W. F.; Alvarez, R. B.; Yuen, T. G. H. J Neurosci Meth 19 (1987) 323-337.

[25] Dymond, A. M.; Kaechele, L. E.; Jurist, J. M.; Crandall, P. H. J Neurosurg 33 (1970) 574-&.

[26] Tseng, T. T.; Monbouquette, H. G. J Electroanal Chem (Lausanne Switz) 682 (2012) 141-146.

[27] Wassum, K. M.; Tolosa, V. M.; Wang, J.; Walker, E.; Monbouquette, H. G.; Maidment, N. T. Sensors 8 (2008) 5023-5036.

[28] Wassum, K. M.; Tolosa, V. M.; Wang, J. J.; Walker, E.; Monbouquette, H. G.; Maidment, N. T. Sensors 8 (2008) 5023-5036.

[29] Yamanaka, K. Jpn J Appl Phys 4 (1898) 632-637.

# Chapter 5: Recommendations for Future Work

## 5.1 PDMS stamping for biosensor fabrication

Future work with this project could focus on increasing the consistency in manufacturing the biosensors so that the sensitivity and limit of detection have a lesser degree of variance. More optimization work could be done to improve the consistency and performance. Parameters could include protein solution inking time, surface drying time after removing the protein solution, surface contact time, depositing chitosan layers in between enzyme layers and using oxygen plasma for PDMS stamp surface treatment.

A crucial, but simple, step in carrying out this procedure is the 'inking' time. Different protein with different properties will result in different inking time. This equilibration time could range from 10 min to 60 min. In general, a small stamp surface will need more inking time to produce consistent protein layers. Since the PDMS surface is hydrophobic, oxygen plasma could oxidize the PDMS stamp surface and generate silanol group (Si-OH). Thus, a hydrophilic surface will be generated for a short time. This will help protein deposition onto the stamp surface. Chitosan could be deposited between protein layers, but it will also increase the impedance. In addition, PPD coating by cyclic voltammetry may give more uniform and stable layers.

The ability to monitor neurotransmitter release in freely behaving animals is key to understanding neuronal processes underlying complex behaviors. Such behaviors are controlled by neuronal networks employing multiple neurotransmitters. There is an extensive literature pointing to the importance of interactions among three neurotransmitters such as dopamine (DA), glutamate (Glut) and acetylcholine (ACh), in controlling the behaviors. [1-4] Thus, it will be very important for biosensors to measure more than one transmitter simultaneously and in near-real

time. By using PDMS stamping, it is possible for us to fabricated biosensors for sensing all of these three neurotransmitters.

Also, by fabricating smaller microelectrodes and microstamps, we could fabricate devices that could measure extracellular potentials as well as DA and Glut release simultaneously. Previous measurement of both the electrophysiological and electrochemical type have been achieved either by switching recording modalities at a single electrode [5-6] or by separate, closely spaced microelectrodes with different modalities [7-8]. The former method has the advantage of sampling both signals from the same location, but does not give us temporal correlation between electrophysiological signaling and electrochemical signaling. The latter approach may be problematic if the two modalities are located in different microenvironments.

The network-level neuronal activity involves not only electrochemical signaling, but also electrophysiological signaling. Actually, microfabricated microelectrode arrays have already been used as a tool for electrophysiological activity recording across multiple spatial locations in the brain. Understanding of the electrophysiological information, such as spikes and field potentials, will be greatly improved if neurotransmitter release could be monitored simultaneously. Although Daryl R. Kipke *et al.* reported simultaneous recording of striatal local potentials, spikes and dopamine release on the same spatiotemporal scale, the number of microelectrodes on the probe is modest and only one neurotransmitter could be detected. [9]

The microcontact printing will be employed here for precise microscale location of enzyme transfer in order to reduce the minimum space between electrodes which will be of great help for device miniaturization and for more precise spatial measurement. The devices could be evaluated for acute studies in awake, head-fixed mice.

## 5.2 Biosensor fabrication by introducing platinum nanograss

A great drawback of current electroenzymatic biosensors is the monitoring of $H_2O_2$ at a high potential (0.7 V vs. Ag/AgCl). Many electroactive interferences in real sample (such as ascorbic acid (AA) etc.) could be oxidized to cause false signals. By using some surface modification materials (such as Pt black) to enlarge the surface area, some reduction in operating potential could be achieved. Pt black is often used for this purpose due to its simple manipulation. However, practical applicability of Pt black is limited as consequence of the low mechanical stability. In addition, Pt-black has been reported to cause cytotoxic reaction due to traces of lead used in the electrolyte during fabrication that may elute from the final coating *in vivo*.

Pt grass will be an excellent substitute of Pt black when coated onto all electrode surfaces for working potential reduction. But the Pt grass deposition time and concentration of the coating solution should be optimized. In addition, we should be careful about the possible corona effect which causes the current drop at the control site. Further investigation of this topic may be interesting.

## 5.3 References


[1] Cepeda, C.; Andre, V. M.; Yamazaki, I.; Wu, N. P.; Kleiman-Weiner, M.; Levine, M. S. Eur J Neurosci 27 (2008) 671-682.

[2] Andre, V. M.; Cepeda, C.; Cummings, D. M.; Jocoy, E. L.; Fisher, Y. E.; Yang, X. W.; Levine, M. S. Eur J Neurosci 31 (2010) 14-28.

[3] Andre, V. M.; Cepeda, C.; Levine, M. S. Cns Neuroscience & Therapeutics 16 (2010) 163-178.

[4] Lapish, C. C.; Seamans, J. K.; Chandler, L. J. Alcohol Clin Exp Res 30 (2006) 1451-1465.

[5] Cheer, J. F.; Heien, M.; Garris, P. A.; Carelli, R. M.; Wightman, R. M. Proceedings of the National Academy of Sciences of the United States of America 102 (2005) 19150-19155.

[6] Crespi, F.; England, T.; Ratti, E.; Trist, D. G. Neurosci Lett 188 (1995) 33-36.

[7] Bickfordwimer, P.; Pang, K.; Rose, G. M.; Gerhardt, G. A. Brain Res 558 (1991) 305-311.

[8] Hefti, F.; Felix, D. J Neurosci Methods 7 (1983) 151-156.

[9] Johnson, M. D.; Franklin, R. K.; Gibson, M. D.; Brown, R. B.; Kipke, D. R. J Neurosci Methods 174 (2008) 62-70.

## Appendix A: Microprobe Fabrication

### *A.1 Fabrication Process Flow Side View*

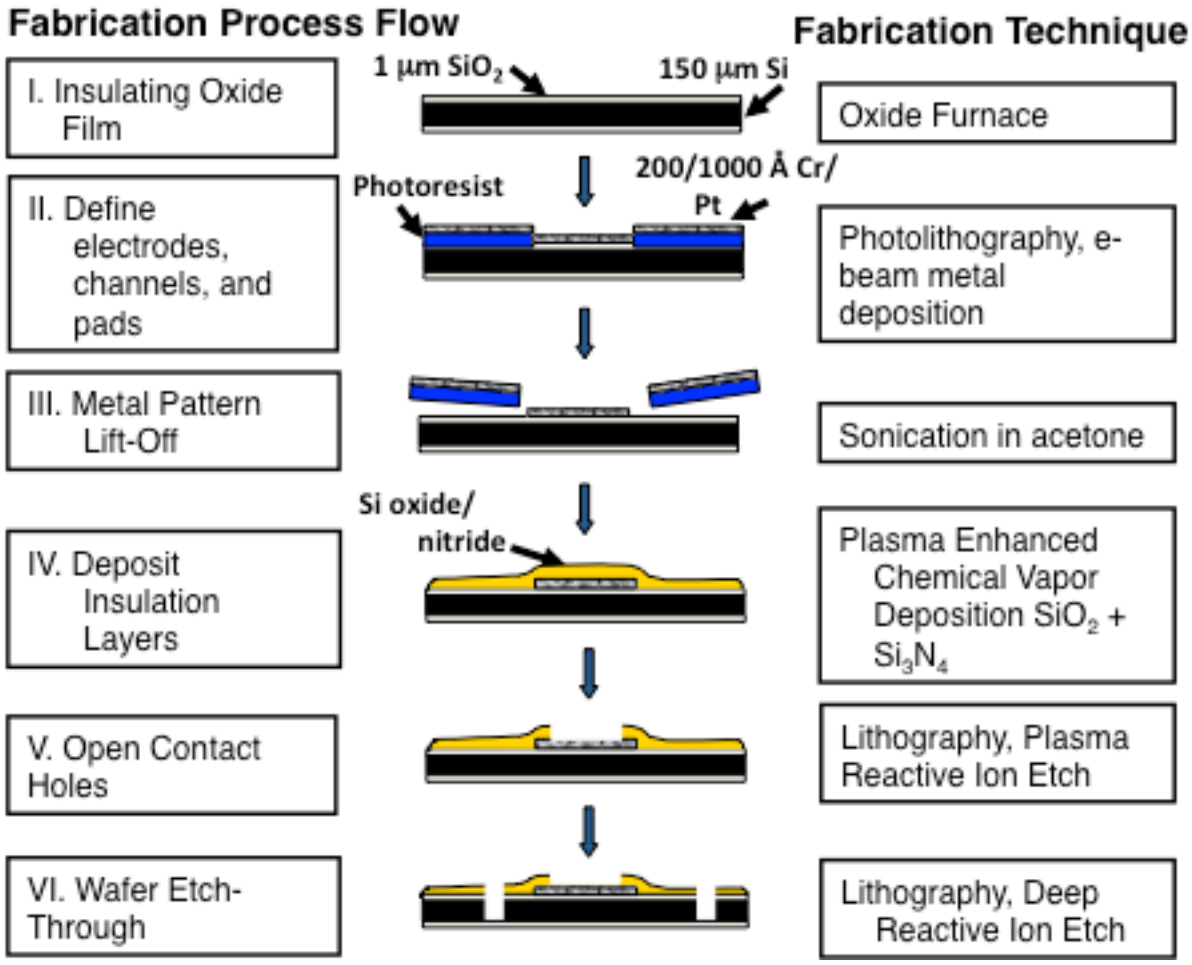


**Figure A.1.** A side profile of the microfabrication process. The individual steps, side profile, and microfabrication techniques are outlined in creating a multielectrode microprobe. A 1 µm-thick layer of silicon dioxide is gronw on a 150 µm-thick silicon wafer using an oxide furnace. The metal deposition step is then done to define the electrodes, leads, and soldering pads. E-beam metal evaporation deposits a thin layer of chromium as a seed layer, followed by 1000 Å of platinum. The photoresist is them removed, leaving behind the patterned metal. The insulation layers are deposited via plasma enhanced chemical vapor deposition, with 750 nm of silicon

dioxide and 750 nm of silicon nitride deposited. Another photolithography step opens up the contact areas over the electrodes and soldering pads. Finally, the sensor outlines are defined in a wafer etch through, which is done via lithography and reactive ion etch.

### *A.2 Materials*

Silicon wafers were ordered from Silicon Valley Microelectronics (Santa Clara, CA) with the following parameters: 100 mm diameter, p-type boron doped, orientation <1 0 0>, 150 μm thickness. All microfabrication was conducted in the Nanoelectronics Research Facility (NRF) at UCLA.

### *A.3 Microfabrication Process Traveler*

| Process | Step | Name | Description | Remarks |
|---|---|---|---|---|
| I. Field oxide formation process | | | | |
| | 1 | Label | Label wafer backside on top/bottom/left/right edges | Use diamond pen<br>Inscribe on the back unpolished side |
| Cleaning Steps | 2 | Piranha bath | Remove organic contaminants:<br>$H_2SO_4$:$H_2O_2$ = 17:1<br>T=70°C; time=10min | Use wafer carrier<br>Refresh solution with 250mL $H_2O_2$ if hasn't been used that day |
| | 3 | Rinse | Time = 2 min | Use rinse cycle in PFC hood |

| | | | | |
|---|---|---|---|---|
| | 4 | HF bath | Remove native oxide:<br>5 sec. HF dip (DIW:HF = 10:1) | Caution. Very corrosive. |
| | 5 | Rinse | Time = 2 min., N2 blow dry after | Gentle water stream<br>Don't use spin dryer (wafers will break) |
| Furnace | 6 | Oxide furnace | Thermally grow 1 μm $SiO_2$<br>Wet recipe (WET1100.001)<br>T=1100 °C, time=2.5 hr | Keep everything clean (gloves/mask on)<br>High temperature (use caution)<br>Use quartz boat. Load wafers ASAP |
| | 7 | Nanospec | Measure $SiO_2$ thickness (Silicon dioxide on silicon) | Measure center/top/bottom/left/ right, average it |
| Cleaning Steps | 8 | Piranha bath | Remove organic contaminants:<br>$H_2SO_4$:$H_2O_2$ = 17:1<br>T=70 °C; time=10 min | Use wafer carrier<br>Refresh solution with 250 mL $H_2O_2$ if hasn't been used that day |
| | 9 | Rinse | Time = 2 min | Use rinse cycle in PFC hood |
| II. Electrode sites, channels, and bonding pads formation | | | | |

| | | | | |
|---|---|---|---|---|
| Lithography I | 10 | Dehydration bake | T=150 °C<br>Time ≥ 5 min | Drive off moisture |
| | 11 | HDMS coat | Improve PR adhesion<br>Time ≥ 5 min | HMDS: hexamethyldisilazane<br>Toxic (operate underneath hood)<br>Do not place wafer in the middle of metal container. Handle dips down and will break wafer when putting cover on. |
| | 12 | Photoresist spin coat | PR: AZ5214-EIR<br>Thickness: ~1.6 μm<br>2500 RPM, Ramp = 1000, time = 30 sec | Clean wafer chuck with acetone<br>Make sure PR covers at least 2/3 of the wafer surface prior to spin |
| | 13 | Soft bake | T=100 °C, time = 1 min. (critical)<br>Place at the center of hotplate | Make sure wafer is flat on hotplate |
| | 14 | Exposure | Karl Suss alignment: | If power varies, use this formula to correct exposure time: |

| | | | | |
|---|---|---|---|---|
| | | | Soft contact, expose for 18 sec (when power = 8 $mW/cm^2$) | t (sec) = 18*(8/actual power in $mW/cm^2$) |
| | 15 | Development | Remove exposed PR<br>5:1 :: DIW:AZ400K developer<br>19 sec. swishing back and forth | 1500 mL DIW : 300 mL AZ400K<br>Use single wafer holder<br>Rinse with DIW for 2 min.<br>Dry with $N_2$ |
| | 16 | Microscope | Inspection | Make sure wafer is fully developed. Do NOT hardbake after this step (for better lift-off results) |
| Metal Deposition | 17 | Metal deposition | Old CHA (evaporated metal deposition)<br>Cr/Pt 200 Å/1000 Å (respectively)<br>Deposition rate: 1Å/sec | Deposit metal within 2 weeks after Litho I<br>Total deposition time: ~3 hrs |
| | 18 | Lift-off | Metal etch: sonicate in acetone (in 2 L beaker) | Use 3 beakers of acetone in series to clean each wafer<br>Keep wafers wet by rinsing with acetone<br>Rinse with DIW and dry with $N_2$ |

| | | | | |
|---|---|---|---|---|
| | 19 | Microscope | Inspection | Check for broken leads, chipped sites |
| III. Insulation layer deposition | | | | |
| Oxide/Nitride Deposition | 20 | PECVD oxide | STS PECVD: 7500 Å<br>Recipe: HFSIOST<br>Time: ~30 min | Blowdry wafer with $N_2$ prior to placing in machine |
| | 21 | Nanospec | Measure $SiO_2$ thickness (Silicon dioxide on silicon)<br>Goal: 7500 Å | Measure center/top/bottom/left/ right<br>Subtract field oxide thickness to calculate deposited thickness |
| | 22 | PECVD nitride | STS PECVD: 7500 Å<br>Recipe: HFSINST<br>Time: ~50 min | |
| | 23 | Nanospec | Measure $Si_3N_4$ thickness (silicon nitride on silicon dioxide)<br>Goal: 7500 Å | Measure center/top/bottom/left/ right<br>For previous oxide thickness, type in average from step #21 |
| IV. Open electrodes/soldering pads | | | | |

| | | | | |
|---|---|---|---|---|
| Lithography II | 24 | Dehydration bake | T=150°C<br>Time ≥ 5 min | Drive off moisture |
| | 25 | HDMS coat | Improve PR adhesion<br>Time ≥ 5 min | HMDS: hexamethyldisilazane<br>Toxic (operate underneath hood)<br>Do not place wafer in the middle of metal container. Handle dips down and will break wafer when putting cover on. |
| | 26 | Photoresist spin coat | PR: AZ5214-EIR<br>Thickness: ~1.6 μm<br>2500 RPM, Ramp = 1000, time = 30 sec | Clean wafer chuck with acetone<br>Make sure PR covers at least 2/3 of the wafer surface prior to spin |
| | 27 | Soft bake | T=100 °C, time = 1 min. (critical)<br>Place at the center of hotplate | Make sure wafer is flat on hotplate |
| | 28 | Exposure | Karl Suss alignment: | If power varies, use this formula to correct exposure time: |

| | | | | |
|---|---|---|---|---|
| | | | Soft contact, expose for 18 sec (when power = 8 $mW/cm^2$) | t (sec) = 18*(8/actual power in mW/cm2) |
| | 29 | Development | Remove exposed PR<br>5:1 :: DIW:AZ400K developer<br>19 sec. swishing back and forth | 1500 mL DIW : 300 mL AZ400K<br>Use single wafer holder<br>Rinse with DIW for 2 min.<br>Dry with $N_2$ |
| | 30 | Microscope | Inspection | Make sure wafer is fully developed. |
| | 31 | Hard bake | T = 150 °C, 5 min.<br>Place at center of hotplate | Do not post bake before inspection<br>Let cool before storing |
| Nitride/Oxide Etch | 32 | Si wafer carrier | Apply moist cooling grease on 500μm Si wafer carrier<br>Bake 3 min @ 75 °C on hotplate | Use q-tips to apply grease in circles over entire surface of carrier wafer<br>Make sure wafer backside is clean of grease<br>Stick wafer onto carrier wafer tightly by placing onto wafer and rotating until flats are aligned |

| | | | | |
|---|---|---|---|---|
| | 33 | Nitride and oxide etch | AOE (recipe: LJYDBOX)<br>Etch time: ~7-8 min. (this etch time may be longer or shorter depending on the status of the AOE) | Remove 1.5 μm of nitride and oxide insulation layer |
| | 34 | Inspection | Voltmeter or Nanospec | Voltmeter: check if resistance between test metal is zero<br>Nanospec: check if thickness of oxide ≤field oxide thickness |
| Cleaning Steps | 35 | PR strip | Matrix stripper<br>3 min. recipe | Make sure to keep wafer stuck to carrier wafer until after this step |
| | 36 | Release carrier | Slide wafer off carefully | Clean wafer backside and carrier wafer with acetone |
| V. Define probe outline | | | | |
| Lithography III | 37 | Dehydration bake | T=150 °C<br>Time ≥ 5 min | Drive off moisture |
| | 38 | Photoresist spin coat | PR: NR9-8000 (negative PR) | Clean chuck with acetone |

| | | | | |
|---|---|---|---|---|
| | | | Thickness: ~12 μm<br>2000 RPM, Ramp: 5000,<br>Time: 30 sec | Make sure PR covers at least 2/3 of wafer surface |
| | 39 | Soft bake (prebake) | T=130 °C, 3 min. (critical)<br>Place at center of hotplate | Make sure wafer is flat on hotplate |
| | 40 | Exposure | Karl Suss alignment:<br>Soft contact, exposure time: 90 sec (power: 8mW/cm$^2$) | If power varies, use this formula to correct exposure time:<br>t (sec) = 90*(8/actual power in mW/cm$^2$) |
| | 41 | Relax | Ambient 5 min | |
| | 42 | Post-exposure bake | T=100 °C, 2 min. (critical)<br>Place at center of hotplate | After bake, let rest for 5 min. |
| | 43 | Development | Developer: RD6<br>3 min. shaking back and forth | Do not dilute RD6 with DI water<br>Rinse with DI water for 2 min. post development<br>Blow dry with $N_2$ |
| | 44 | Microscope | Inspection | Make sure wafer is fully developed |

| | | | | |
|---|---|---|---|---|
| Si Wafer Etch-Through | 45 | SiO2 wafer carrier | Apply moist cooling grease on 500μm thick $SiO_2$ carrier wafer<br>Bake 3 min. @ 75 °C | Use q-tips to apply grease in circles over entire surface of carrier wafer<br>Make sure wafer backside is clean of grease<br>Stick wafer onto carrier wafer tightly by placing onto wafer and rotating until flats are aligned |
| | 46 | Nitride/oxide etch | AOE (recipe: LJYDBOX)<br>Etch time: ~7-8 min. (this etch time may be longer or shorter depending on the status of the AOE) | Remove all nitride and oxide from exposed areas |
| | 47 | Inspection | Voltmeter: Si test square at bottom | Resistance is ~16 MΩ if all oxide and nitride is removed |
| | 48 | Si etch through | DRIE (deep reactive ion etch):<br>Recipe 59BOSCH<br>~72 min. total etch time (this etch time may be | Do not run DRIE for more than 30 minutes at a time (could overheat the wafer) |

| | | | | |
|---|---|---|---|---|
| | | | longer or shorter depending on the status of the DRIE) | If getting pressure error, run an $O_2$ plasma clean for 30 min |
| | 49 | Inspection | Microscope | Do not release wafer from carrier until etch through of silicon is confirmed. Should be able to see cooling grease through the outlines for silicon etch through |
| Stripping PR | 50 | Release carrier | Slide wafer off carefully | Clean carrier with acetone |
| | 51 | PR strip | PR stripper sink (ALEG 355)<br>T=75 °C, at least 30 min. | Rinse with DI water for 2 min. after<br>Blow dry with $N_2$ |

## Appendix B: Preparing Glucose Sensors from Disk Electrode

### *B.1 Materials*

- Pyrrole, reagent grade 98% (Sigma 131709)
- Nafion® perfluorinated resin solution, 5 wt. % in lower aliphatic alcohols and water (Sigma 274704)
- Glucose oxidase (Sigama)
- Glutaraldehyde solution, 25% in water (Sigma G5882)
- Albumin from bovine serum, lyophilized powder, ≥96% (Sigma A4503)

### *B.2 Pre-Procedure*

- 200 mM pyrrole: 140 μL of pyrrole was mixed into 10 mL of PBS. This mixture was shaken well.
- Glucose oxidase aliquot: Dissolve GOx at a concentration of 20 mg/mL PBS. Centrifuge the bottle so all liquid is at the bottom.
- BSA solution: Dissolve 20 mg BSA in 1 mL DI water.
- Pre-heat oven to 180 °C.
- Polydimethylsiloxane (PDMS) stamps: Fabricated using the Sylgard® 184 silicone elastomer kit from Dow Corning. The curing agent and monomer were mixed at a 1:10 ratio in a Petri Dish to give a ~2-mm-thick polymer film. Subsequently, the mixture was carefully degassed under vacuum and cured at 60 ℃ for 4 hrs. A cylindrical feature of ~1.6 mm diameter and ~2 mm height was punched from the film and a rectangular PDMS support (~5 mm square) was cut as well. Next, the cylindrical PDMS piece was glued at

the center of the rectangular piece using an uncured mixture of curing agent and base monomer. The assembled PDMS stamp was ready after curing at 60 ℃ for 4 hours.

- The pH of the chitosan solution (0.04% m/v) was adjusted to pH 3 using hydrochloric acid (HCl) to dissolve the chitosan flakes. (Overnight)

***B.3 Procedure***

1. The Pt disk electrode (1.6 mm dia.) was polished using a microcloth with a 0.05 μm particle suspension. After rinsing with ultrapure water, it was sonicated in isopropyl alcohol followed by electrochemical cleaning with 0.5 M sulfuric acid and ultrapure water, respectively.
2. a polypyrrole (PPy) film was electrodeposited (200 mM Py in stirred PBS, 0.85 V *vs.* Ag/AgCl, ~5 min) onto the Pt surface
3. Nafion dip-coating with a 5% Nafion® solution and baking in an oven at 180 ℃ for 3 min (Repeat once)
4. Chitosan solution: After filtering with a 0.2 μm syringe filter, the pH was adjusted to 5 using sodium hydroxide (NaOH) solution (0.5 M).
5. A constant potential of -0.7 V *vs.* Ag/AgCl was applied at the PPy/Nafion-coated Pt electrode surface for 2 min while immersed in the chitosan solution to electrodeposit a chitosan film. (Repeat twice)
6. A droplet of GOx/BSA solution, mixed in a 1:1 mass ratio (Final Concentration: BSA: 10 mg/mL; GOx 10 mg/mL) in PBS, was placed on the cleaned PDMS stamp surface and left at room temperature for ~10 min (inking time).

7. The excess protein solution was carefully wicked from the stamp with a Kimwipe, and the stamp was dried under a stream of argon for ~30 s.
8. The stamp then was placed horizontally in contact with the chitosan-coated electrode surface for 10-15 s.
9. Subsequently, the disk electrode surface was exposed to the vapor from a 12.5% GAH solution at room temperature for 45 sec.
10. Sensor stored at 4 °C in dessicant overnight.
11. Quantification of immobilized glucose oxidase

(1) Make standard FAD solutions. The FAD solutions were stored in the dark until use.

(2) A calibration curve was created from recordings of the fluorescence intensity of various concentrations of FAD in an aqueous solution of 8 M urea and 0.05 M KCl.

(3) The emission intensity at 525 nm scaled linearly with the FAD concentration between 19.2 nM and 1229.7 nM at an excitation wavelength of 375 nm.

(4) Enzyme-coated electrodes were soaked in 0.7 mL of 8 M urea solution overnight to ensure that FAD was leached completely from the electrode surface. The emission intensity at 525 nm was then measured and correlated to enzyme concentration using the calibration curve described above.

## Appendix C: Preparation of Microstamp Mold

### *C.1 Procedure*

1. SU-8 2075 was spin-coated on top of a 4 inches Si wafer at 2000 rpm for 30 s for ~ 100 μm thick layer.
2. The layer was soft-baked at 65 ℃ for 5 min and then at 95 ℃ for 40 min followed by UV exposure of 216 mJ/cm$^2$.
3. Post exposure bake was done at 65 ℃ for 5 min and at 95 ℃ for 10 min.
4. After the layer was patterned in SU-8 developer for 20 min, Afterwards, the mold was cleaned using isopropanol and then left to dry in the air at room temperature.
5. Polydimethylsiloxane (PDMS) microstamps were fabricated using the Sylgard® 184 silicone elastomer kit. To cover a 4 inch mold, 6 g of monomer was mixed with 0.6 g of curing agent (1:10; monomer:curing agent) and then centrifuged at 15000 rpm for 5 min to remove air bubbles.
6. After pouring onto the SU-8 mold, the mixture was subsequently degassed under vacuum and cured at 60 ℃ for 4 h.
7. The PDMS microstamps were detached from the mold and cut into 1 cm × 1 cm pieces for stamping.
8. To ensure that the enzyme mixture is transferred to the entire microelectrode surface (40 μm × 150 μm), the size of a microstamp surface was designed to be 50 μm × 160 μm.
9. The PDMS stamps were cleaned in 7.5 % hydrogen peroxide with sonication and then re-used.

## Appendix D: Preparation of Glucose and Choline Sensor from Microelectrode

### *D.1 Materials*

Glucose oxidase (from *Aspergillus niger*, CAS NO. 9001-37-0), pyrrole (Py), Choline oxidase (Alcaligenes, 9028-67-5), m-phenylenediamine (PD), Choline chloride, glutaraldehyde solution (25%), bovine serum albumin (BSA) lyophilized powder, hydrogen peroxide solution (30%), chitosan (From crab shells, minimum 85% deacetylated), D-(+)-glucose, L-ascorbic acid, dopamine hydrochloride, potassium hexacyanoferrate (II) trihydrate, and potassium hexacyanoferrate (III) were purchased from Sigma-Aldrich (St. Louis, MO). Isopropyl alcohol and 1M sulfuric acid solutions were obtained from Fisher Scientific (Pittsburgh, PA).

### *D.2 Procedure*

1. Microelectrodes were rinsed with isopropyl alcohol followed by an electrochemical cleaning step with 0.5 M sulfuric acid and sonicated in ultrapure water.
2. Polyphenylenediamine (PPD) film was electrodeposited (5 mM PD in stirred PBS, 0.85 V *vs.* Ag/AgCl, 10 min) onto the electrode surface.
3. The pH of the chitosan solution (0.04% m/v) was adjusted to pH = 3 using hydrochloric acid (HCl) to dissolve the chitosan flakes. After filtering with a 0.2 μm syringe filter, the pH was adjusted to 5 using sodium hydroxide (NaOH) solution (0.5 M). A constant potential of -0.7 V *vs.* Ag/AgCl was applied at the PPD-coated Pt electrode surface for 2 min while immersed in the chitosan solution to electrodeposit a chitosan film.
4. A droplet (3 μL) of enzyme mixture was placed on a PDMS microstamp for ~ 60 min. ChOx (17.5 mg/mL) and GOx (10 mg/mL) were mixed with bovine serum albumin (BSA)

in a 1:1 mass ratio in phosphate-buffered saline (PBS) for choline and glucose sensing sites, respectively.

5. After inking, the excess enzyme solution was removed using a Kimwipe, then the microstamp was dried using a nitrogen gun for ~ 15 s.
6. There is an array of electrodes (2 × 2) on a microprobe and the separation of the electrodes were measured to be 40 μm and 105 μm in the x and y-direction, respectively. The alignment setup consists of a microscope and a separate stage. A microstamp fixed on a stage was focused by a separate microscope.
7. The microstamp was attached to the stage and focused by the the separate microscope where a target microprobe was fixed.
8. Alignment of the PDMS microstamp and the target microelectrode was done by moving the microscope stage.
9. The microscope stage was then raised to make contact with the PDMS microstamp. ChOx mixture and GOx mixture were respectively stamped on selected microelectrode surface.
10. The microprobe was exposed to vapor from 5% glutaraldehyde (GAH) solution at room temperature for 1 min. (Repeat once)
11. The fabricated sensors were preserved at 4 ℃ under dry conditions when not in use.

## Appendix E: Pt Nanograss Coated Choline Sensor Fabrication

### *E.1 Materials*

Choline oxidase (Alcaligenes, 9028-67-5), m-phenylenediamine, Nafion® (5%), glutaraldehyde solution (25%), bovine serum albumin (BSA) lyophilized powder, 3,4-

dihydroxyphenylacetic acid, 3,4-dihydroxy-DL-phenylalanine, (-)-epinephrine (+)-bitartrate salt, DL-norepinephrine hydrochloride, serotonin hydrochloride, hydrogen peroxide solution (30%), choline hydrochloride, D-(+)-glucose, iridium tetrachloride hydrate, oxalic acid dehydrate (99%); L-ascorbic acid, dopamine hydrochloride, formic acid, chloroplatinic acid hexahydrate were purchased from Sigma-Aldrich (St. Louis, MO).

### *E.2 Procedure*

1. Pt nanograss solution: aqueous solution of 2.5 mM $H_2PtCl_6$ and 1.5 mM formic acid (1X, for working electrode modification) and 25 mM $H_2PtCl_6$ and 15 mM formic acid (10X, for reference electrode deposition).
2. Pt-grass formation was conducted potentiostatically from the $H_2PtCl_6$ solution at a potential of -0.1 V vs Ag/AgCl for 300 s.
3. For Pt black deposition, a Pt black layer was deposited on the cleaned electrodes by cycling potential between 1.4 and 2.0 V at 500 mV/s for a total of 15 cycles in a vigorously stirred plating solution. The plating solution consisted of 1% chloroplatinic acid, 0.0025% HCl, and 0.01% lead acetate in water, which was Ar-purged for 15 min.
4. PPD was electrodeposited from a stirred solution of 5 mM PD in PBS (pH 7.4) by holding the voltage constant at 0.85 V for 5 min.
5. Nafion was deposited on all sites by rapid dip-coating of the probe tips in the Nafion solution and oven-casting at 175 $^{o}$C for 4 min, followed by a 3-min cooling period in ambient air.
6. Enzyme immobilization by chemical crosslinking was accomplished using a solution consisting of ChOx (0.33unit/uL), BSA (20ug/uL) and glutaraldehyde ($5 \times 10^{-3}$ uL/uL).

7. A small drop of the solution was formed on a syringe tip and the drop was gently swiped across the bottom two microelectrode sites at the probe tip under microscope. This swipe was repeated eleven more times.
8. The biosensors were sealed in a container with desiccant and stored dry at 4 $^{o}$C for 48 h prior to testing.